

THESIS FOR THE DEGREE OF DOCTOR OF PHILOSOPHY

Chloride Induced Corrosion of Reinforcement Steel in Concrete

Threshold Values and Ion Distributions at the Concrete-Steel Interface

NELSON SILVA

Department of Civil and Environmental Engineering

CHALMERS UNIVERSITY OF TECHNOLOGY

Gothenburg, Sweden, 2013

Chloride Induced Corrosion of Reinforcement Steel in Concrete
Threshold Values and Ion Distributions at the Concrete-Steel Interface

NELSON SILVA

ISBN 978-91-7385-808-3

© NELSON SILVA, 2013

Doktorsavhandlingar vid Chalmers tekniska högskola
Ny serie nr 3489
ISSN 0346-718X

Department of Civil and Environmental Engineering
Division of Building Technology
Chalmers University of Technology
SE-412 96 Göteborg
Sweden
Telephone + 46 (0)31-772 1000
www.chalmers.se

Chalmers Reproservice
Göteborg, Sweden 2013

Chloride Induced Corrosion of Reinforcement Steel in Concrete

Threshold Values and Ion Distributions at the Concrete-Steel Interface

NELSON SILVA

Department of Civil and Environmental Engineering

Division of Building Technology

Chalmers University of Technology

Abstract

The chloride threshold value (C_{th}), or critical chloride content, is defined as the chloride concentration at the depth of the reinforcement, which initiates the depassivation of steel in concrete. However, very limited information is available regarding the chloride distributions at the interface with the steel. The main objective of this work is to improve the knowledge and understanding about the mechanisms leading to depassivation of steel in concrete, by studying the influence of the steel surface condition and the concrete-steel interface on the corrosion initiation and the chloride distributions along the concrete-steel interface at the time of depassivation.

Laser ablation inductively coupled plasma mass spectrometry (LA-ICP-MS) was used for spatial resolved chloride profiling in cementitious materials. A range of materials with increasing degree of heterogeneity (i.e. cement paste, mortar and concrete) and exposed to chlorides under different conditions (i.e. mixed-in, diffused and migrated) was studied. The system was optimized for maximum chloride sensitivity, while allowing for the detection of other elements such as calcium and iron. At a scan speed of 100 $\mu\text{m/s}$, a spatial resolution of 300-400 μm and limits of detection of 0.05 wt% of cement were determined.

The chloride distributions along the concrete-steel interface and possible differences between passive and active regions were studied, for different steel surface conditions under free corrosion conditions as well as under potentiostatic control. The results have shown that along the interface, a range of chloride concentrations can be expected, with higher values around the corroding active sites. It was suggested that chlorides preferentially accumulate at the anodic regions even prior to depassivation, leading to pitting corrosion. A local migration mechanism was proposed to account for the chloride build-up around the anode regions, due to the formation of local potential gradients on the passive layer of the steel as a result of differences in the moisture content and oxygen availability, concentration of aggressive species and metallurgical properties, such as inclusions or mill-scale along the steel. In particular the steel surface condition and the presence of air voids at the concrete-steel interface were recognized as major factors influencing the development of potential gradients along the steel surface.

Keywords: LA-ICP-MS, concrete-steel interface, chloride threshold values, pitting corrosion.

Contents

Abstract	i
Preface	v
Acknowledgments	vii
List of papers	ix
Other publications	x
Abbreviations	xi
1 Introduction	1
1.1 Background	1
1.2 Objectives and limitations	1
1.3 Outline of the thesis	2
2 Theoretical background	5
2.1 Chloride transport in concrete	5
2.2 Corrosion of steel in concrete	7
2.2.1 Thermodynamics and pitting corrosion	7
2.2.2 Electrochemical measurement techniques	11
2.2.3 Electrochemical rehabilitation methods	14
2.3 Corrosion initiation and chloride threshold values	16
2.3.1 Surface condition of the steel	16
2.3.2 Concrete-steel interface	17
2.3.3 Pore solution and binder type	19
2.4 Chloride content measurement	20
2.4.1 Current practice and techniques	20
2.4.2 LA-ICP-MS innovative approach	21
3 Experimental work	23
3.1 LA-ICP-MS method development	23
3.1.1 Reference materials	23
3.1.2 Operating conditions	24
3.2 Chloride distributions and steel surface condition	24
3.2.1 Materials	24
3.2.2 Methods	25
3.3 Chloride distributions at the time of depassivation	26
3.3.1 Materials	26

3.3.2	Methods	29
4	Results and discussion	31
4.1	LA-ICP-MS method development	31
4.2	Chloride distributions and steel surface condition	33
4.3	Chloride distributions at the time of depassivation	35
5	Conclusions	41
6	Future research	43
7	References	45
Appended Papers I-V		

Preface

This doctoral thesis is submitted to Chalmers University of Technology (CTH) as a partial fulfilment of the requirements for the degree of Philosophiae Doctor (PhD). It consists of papers published in, and submitted to, scientific journals.

The major part of work has been carried out at the Division of Building Technology, Department of Civil and Environmental Engineering, Chalmers University of Technology, in close collaboration with CBI Cement and Concrete Research Institute. At the final stage of the project, one part of the experimental work was carried at the Department of Earth Sciences, University of Gothenburg.

Main supervisor has been Professor Tang Luping (CTH) and co-supervisors have been Dr. Jan Erik Lindqvist (CBI) and Associate Professor Sébastien Rauch (CTH).

The project started in February 2009 and completed for submission in January 2013.

Acknowledgements

FORMAS, the Swedish Research Council for Environment, Agricultural Sciences and Spatial Planning is acknowledged for financing this project.

First of all I would like to thank my main supervisor, Tang Luping, for changing my life by giving me the opportunity to move to Sweden. Your endless patience, motivation and assertiveness have made this work possible. I have learnt immensely under your guidance, both technically and personally.

To my co-supervisor, Jan Erik Lindqvist, for sharing all your vast knowledge in the field of microscopy, for the critical comments and discussions on the experiments and results and especially for helping me “draw the line”.

To my co-supervisor, Sébastien Rauch, for all your support concerning the LA-ICP-MS technique.

To Dimitrios Boubitsas, for your valuable co-operation and fruitful discussions.

To Marek Machowski, for all your help both in and out of the lab.

To Johan Hogmalm, for your help with the LA-ICP-MS in Paper V.

To Paula Wahlgren, for your reasoning, especially in the final stage of this project.

To all my colleagues at the Division of Building Technology for contributing for a peaceful and creative work environment.

To all my family and friends in Sweden for your warm presence.

Gostaria ainda de agradecer todo o apoio da minha família e amigos em Portugal.

Aos meus pais, Adília Silva e Fernando Silva: Obrigado, amo-vos muito!

E finalmente, para a minha VIDA, Eva Rocha: Sem ti, nada disto faria sentido!

Nelson Silva

Gothenburg, January 2013

List of papers

This thesis includes the following appended papers which are referred throughout the text by their Roman numerals:

- I Application of LA-ICP-MS for meso-scale chloride profiling in concrete**
N. Silva, T. Luping and S. Rauch
Materials and Structures (2012) DOI: 10.1617/s11527-012-9979-y

- II Chloride profiles along the concrete-steel interface**
N. Silva, T. Luping, J.E. Lindqvist and D. Boubitsas
International Journal of Structural Engineering Vol.4, Nos. 1/2 (2013) 100-112

- III Critical conditions for depassivation of steel in concrete: Interface chloride profiles and steel surface condition**
N. Silva, D. Boubitsas, T. Luping and J.E. Lindqvist
Nordic Concrete Research 45 (2012) 111-123

- IV Chloride profiles at the concrete-steel interface with different initial steel surface conditions**
N. Silva, D. Boubitsas, T. Luping and J.E. Lindqvist
Submitted to *Cement and Concrete Research*

- V Chloride profiles at the concrete-steel interface at the time of corrosion initiation and threshold values**
N. Silva, J. Hogmalm, T. Luping and J.E. Lindqvist
Submitted to *Corrosion Science*

Other publications

In addition to papers I-V, the following publications resulted from the work carried out in the present PhD project. These publications are not appended to the present thesis.

- I An innovative approach to measure chloride threshold levels in reinforced concrete**
N. Silva, T. Luping and S. Rauch
In: *Modelling the Durability of Reinforced Concrete*, RILEM Proceedings PRO69. Eds: R.M. Ferreira, J. Gulikers and C. Andrade, RILEM Publications S.A.R.L., 2009, pp.28-34.
ISBN 978-2-35158-095-0.

- II Chloride contents at the concrete-steel interface**
N. Silva, T. Luping, J.E. Lindqvist and D. Boubitsas
In: *Advances in Concrete Structural Durability*, Proceedings of ICDCS2010. Eds: H. Yokota, T. Sugiyama and T. Ueda, Hokkaido University Press, 2010, pp.275-284.
ISBN 978-4-8329-0360-9.

- III Critical conditions for depassivation of steel in concrete: interface chloride profiles**
N. Silva, T. Luping, J.E. Lindqvist, and D. Boubitsas
In: *Nordic Concrete Research*, Proceedings of the XXI Nordic Concrete Research Symposium. Ed: Nordic Concrete Federation, No.43, 2011, pp.115-118.
ISBN 978-82-8208-025-5.

- IV Chloride analysis in concrete by LA-ICP-MS**
N. Silva, T. Luping and S. Rauch
In: *Advances in Construction Materials through Science and Engineering*, RILEM Proceedings PRO79. Eds: C. Leung and K.T. Wan, RILEM Publications S.A.R.L., 2011, p.137.
ISBN 978-2-35158-116-2.

Abbreviations

The following is a general list of abbreviations used throughout the chapters in this thesis. Specific symbols and abbreviations have been used in the appended papers.

CP	Cathodic protection
CPre	Cathodic prevention
CSH	Calcium silicate hydrates
C_{th}	Chloride threshold value (critical chloride content)
ECE	Electrochemical chloride extraction
E_{corr}	Corrosion potential
EDS	Energy dispersive spectrometry
E_{pit}	Pitting potential
EPMA	Electron probe micro analyser
ER	Electrochemical realkalization
ET	Electrochemical treatment
FA	Fly ash
FRP	Fiber reinforced polymer
GGBS	Ground granulated blast furnace slag
LA-ICP-MS	Laser ablation inductively coupled plasma mass spectrometry
LIBS	Laser induced breakdown spectroscopy
LOD	Limit of detection
NIR	Near-infrared spectrometry
PC	Portland cement
RH	Relative humidity
SCC	Self compacting concrete
SCE	Saturated calomel electrode
SEM	Scanning electron microscopy
SF	Silica fume
SHE	Standard hydrogen electrode
w/b	Water binder ratio
wt%	Weight percentage
XRD	X-ray diffraction
XRF	X-ray fluorescence spectrometry

1 Introduction

1.1 Background

Reinforced concrete is one of the most widely used building materials. It is relatively cheap, due to the availability of raw materials, versatile, allowing a wide range of forms and applications and durable if designed and executed in a proper way. However, the ingress of external agents such as carbon dioxide, chloride ions or sulphates, will eventually lead to degradation. The main cause for deterioration of reinforced concrete structures is the corrosion of the embedded steel, in particular when exposed to marine environments or de-icing salts, due to the action of chloride. The service life of reinforced concrete structures is, according to the classic model by Tuutti (1982), divided into two periods: initiation and propagation. Initiation is defined as the period until depassivation of steel is detected. In order to properly design this period, knowledge of the chloride ingress rate and the critical condition for depassivation is necessary. The propagation period on the other hand, requires knowledge of the corrosion rate so as to be able to make predictions concerning the structural integrity.

The critical condition for depassivation is most often expressed in terms of the chloride threshold value (C_{th}) or critical chloride content. The topic of C_{th} was initiated in the 1950's and according to the most recent literature review by Angst et al. (2009a), C_{th} values range from 0.04 wt% to 8.34 wt% of cement. With such large scatter is almost impossible to define appropriate criteria for service life design. The main reason for such variation is the number of parameters with influence on the corrosion initiation (e.g. binder type, water-binder ratio, type of steel, etc.). In addition, the different methods used in the experiments make comparison of the results difficult. The recently created RILEM TC 235 CTC (2009) is a unified effort to try to clarify terminologies and procedures that can be widely accepted. However, it is worth to notice that, even upon agreement of a test method, variability in C_{th} is to be expected because pitting corrosion is strongly dependent on the microenvironment at the concrete-steel interface.

While the microstructure of the concrete-steel interface and the surface finish of the steel are widely recognized to influence the corrosion initiation, no systematic investigation has been performed as to what concerns the chloride distributions at the pitting positions and their relationship with the chloride content measured in the surrounding concrete. Therefore, it is still unknown if at the time of depassivation, the chloride content is locally higher and if so, the reasons for it.

1.2 Objectives and limitations

The aim of this work is to improve the knowledge and understanding about the mechanisms leading to depassivation of steel in concrete exposed to chlorides, by studying the following three points:

1. Measurement of the total chloride content in cementitious materials by developing a scanning method with meso-scale resolution (in a range of 0.01 to 1 mm). This

involved optimization of the analytical settings in order to guarantee linear behaviour and low limits of detection (0.05 wt% of cement), while maintaining high sensitivity to other elements such as calcium and iron. This work is summarised in Paper I.

2. Application of the method developed in the first point to the study of the chloride distributions along the concrete-steel interface. Possible differences between passive and active regions are investigated considering, different steel surface conditions, the effect of air voids at the interface and open circuit potential as well as potentiostatic control. This point generated Papers II, III and IV.
3. To study the mechanism of chloride induced reinforcement corrosion, by investigating the chloride distributions along the interface, similar to point number 2, but at the time of depassivation. Furthermore, the study was limited to one type of steel surface under free corrosion conditions. The main results are discussed in Paper V.

In this study, concrete is considered submerged or exposed in the tidal zone. Interfacial air voids are considered in the unsaturated condition. Carbonation is not taken in consideration. In the final part of the project both the effect of additions and electrochemical treatment is accounted for, in the experimental determination of chloride threshold values. It was initially idealized to correlate the meso-scale chloride content along the interface, at the time of depassivation, with that measured by traditional powder sampling of the bulk concrete. However, sometime between points 2 and 3, the LA-ICP-MS equipment at Chalmers was disabled and thereon only qualitative studies were undertaken (point 3, Paper V).

1.3 Outline of the thesis

This thesis consists of an introductory part composed by seven chapters, including a reference list, and five papers.

Chapter I is an introduction intended to present the background of the project as well as the objectives and limitations.

Chapter II gives an overview of the theoretical background considered relevant, with regard to the present thesis, for the discussion of the mechanisms of chloride induced reinforcement corrosion in concrete.

Chapter III summarises the experimental work in the thesis which was divided in three parts and provided the basis for Papers I to V.

Chapter IV summarises the main results and discussions from the project. More specific results are presented in the appended papers.

Chapter V presents both general and specific conclusions of the project.

Chapter VI gives some suggestions for future work based on the experience gained during the course of the project.

Chapter VII is the reference list.

Paper I describes the development of the LA-ICP-MS method for chloride analysis in cementitious materials, which constituted the main working tool of this project. Calibration

strategy, validation against macro-scale measurements and application examples for the analysis of materials of increasing complexity are presented.

Paper II presents the first semi-quantitative results from the application of the LA-ICP-MS method to the study of the chloride distributions along the interface, including differences between corroded and non-corroded sections. The results are validated against EDS measurements. Furthermore, microstructural features and corrosion products are investigated.

Paper III makes a preliminary analysis of factors influencing the corrosion initiation and ion distributions along the interface, based on a limited set of samples for one type of steel surface under free corrosion conditions.

Paper IV analyses the heterogeneous nature of the chloride distributions along the interface and the influence of different steel surface conditions on the depassivation of steel in concrete. A mechanism is proposed as for why air voids act as preferential sites for initiation. Finally, differences between open circuit and potentiostatic control tests are discussed in terms of the average chloride content along the interface.

Paper V studies the chloride distributions along the interface at the time of depassivation and discusses the mechanism leading to the accumulation of chlorides at anodic regions along the concrete-steel interface with regard to the electrochemical potential. In addition, it also examines the influence of the electrochemical treatment on the corrosion initiation.

2 Theoretical Background

This chapter gives an overview of the theoretical background considered relevant for the discussion of the mechanisms of chloride induced reinforcement corrosion in concrete. Section 2.1 focuses on the ingress of chlorides and oxygen in concrete, as these species are fundamental in the corrosion process. Aspects such as pore structure, chloride binding and moisture state are briefly discussed as they influence the transport properties. Section 2.2 deals with the fundamentals of electrochemistry of steel in concrete. It covers aspects such as passivity and mechanisms of pitting corrosion, thermodynamics of corrosion of steel in concrete, electrochemical measurement techniques and electrochemical rehabilitation methods. Under the topic of chloride threshold values, Section 2.3 focuses on the influence of the concrete-steel interface, reinforcement surface condition and some other parameters, in the corrosion initiation. Finally Section 2.4 gives a review of the current practice and an introduction of a new approach for measuring the chloride content in concrete.

2.1 Chloride transport in concrete

Concrete is a porous material as a result of the cement hydration and the pore structure dependent on several factors such as the water-cement ratio or curing temperature (Neville 1995). Three main types of pores are identified: gel pores (ranging from 1 to 10 nm); capillary pores (ranging from 10 nm to 10 μm) and macro pores and air voids (from 10 μm up to several mm). Because of the small size, gel pores do not significantly contribute to transport processes and usually are not considered with regard to durability of the reinforcement (Bertolini et al. 2004). Also macro pores and air voids are often considered to have little influence in the chloride ingress, at least in terms of sorption characteristics. They can however contribute to an increase in the transport rate by gravitation. In any case, the presence of air voids at the concrete-steel interface has been found to strongly influence the resistance to chloride induced corrosion (Yonezawa et al. 1988). The transport and fixation of moisture, ions and gases relevant to the corrosion process is thus strongly dependent on the amount of capillary pores and the degree of interconnectivity between them, i.e. the permeability.

The main mechanisms for chloride transport in concrete are capillary suction, diffusion and migration. Capillary suction occurs for dried or partially dried concrete, when it comes in contact with water (and dissolved ions), due to the surface tension in the capillaries. This is an important mechanism for marine concrete in the tidal and splash zone as well as in the case of concrete in road applications where de-icing salts are used (Bertolini et al. 2004). When concrete is saturated such as in submerged conditions, diffusion is the relevant mechanism for chloride transport. Diffusion occurs due to concentration gradients. For non-steady-state conditions, such as in the case of concrete, where the concentration gradient changes with time, the flux can be described according to Fick's second law of diffusion (equation 2.1):

$$\frac{\partial c}{\partial t} = D \frac{\partial^2 c}{\partial x^2} \quad (2.1)$$

Here, c is the chloride concentration, t is the time, D is the diffusion coefficient and x is the depth. Assuming constant D , the mass balance is usually solved by applying the error function solution (equation 2.2, Collepardi 1972):

$$c(x,t) = c_i + (c_s - c_i) \left[1 - \operatorname{erf} \left(\frac{x}{2\sqrt{D \cdot t}} \right) \right] \quad (2.2)$$

Here c_i is the initial chloride content in concrete and c_s is the surface chloride concentration. When compared to capillary suction, diffusion is a relatively slow process. In the practice however, many models for chloride ingress are still based on Fick's second law of diffusion (Nilsson et al. 1996, Nilsson 2009), although recognising that capillary suction is important in the transport of chloride within the first few millimetres of the concrete cover. In order to account for the time-dependency of the diffusion coefficient, such type of models, describe D in equation (2.2) according to a relationship of the type (equation 2.3, Takewaka and Matsumoto 1988, Tang and Nilsson 1992, Mangat and Molloy 1994):

$$D(t) = D_0 \cdot \left(\frac{t_0}{t} \right)^n \quad (2.3)$$

Here, D_0 is an apparent diffusion coefficient at a reference time t_0 and n is the age factor, a constant dependent on the type of binder or water-cement ratio. In Nilsson (2009) and in Tang et al. (2012), a number of other models are reviewed. Finally, migration is defined as the transport of ions under the action of an electrical field. The velocity of the migrating ion depends on the strength of the electrical field and the size and charge of the ion. Electrical fields may be present in concrete when electrochemical techniques are used, e.g. cathodic protection, when electrochemical potential gradients along the steel surface exist, e.g. localized corrosion cells or due to diffusion potentials arising from movement of different ionic species (Angst and Vennesland 2009, Angst et al. 2009b, Angst et al. 2010).

Transport processes are strongly influenced by the relative humidity. While chloride ions require a continuous liquid phase in the pore system to diffuse, oxygen transport is higher at low relative humidity. The diffusion rate of chloride ions in concrete is thus highest at saturation or close to it and negligible at relative humidity below 50% (Nielsen and Geiker 2003). On the contrary, oxygen diffusivity strongly decreases when $RH > 70\%$ since oxygen has to diffuse through the water in the pores, a much slower process than in empty air-filled pores. Figure 2.1 schematically illustrates how the diffusion of chloride and oxygen is influenced by the relative humidity.

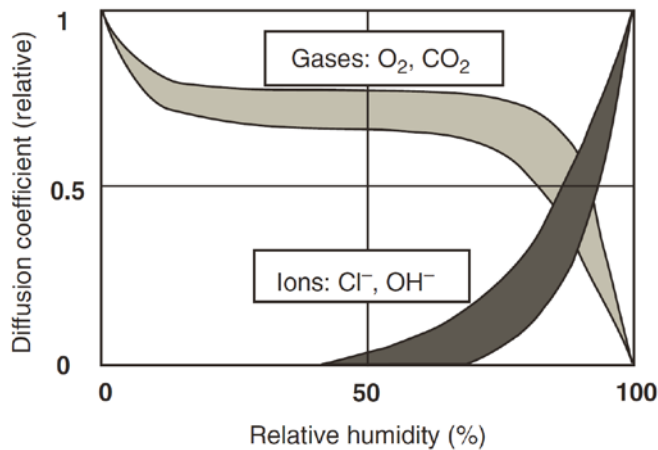


Figure 2.1. Influence of the relative humidity in the diffusion coefficient of gases and ions (Hunkeler 2005).

In addition to the influence of the moisture conditions, the rate of chloride ingress in concrete is also affected by the interaction of chloride with the cement paste. Chemically, chloride can bind with the aluminate phases of the cement to form Friedel's salt (Nagataki et al. 1993), while physically they can be adsorbed on the pore walls (Nilsson et al. 1996). Physical and chemical chloride binding can effectively delay the chloride transport through concrete and the corrosion onset, as only free chlorides interact with the reinforcement. However, they can also represent an extra source of chloride if for example, the temperature changes or the pH of the pore solution drops due to carbonation. A review on the importance of bound and free chlorides on the chloride threshold levels for corrosion initiation is given by Glass and Buenfeld (1997).

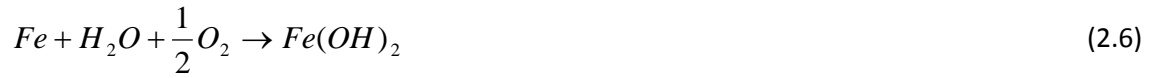
Finally, it is worth mentioning that concrete always contain cracks that can to more or less extent affect the transport properties. Cracks are present in concrete even from early ages as a result of e.g. plastic shrinkage and may be induced or propagate (both in length and width) during the service life of a structure due to e.g. mechanical loading. Depending on the width, cracks may provide preferential paths for ingress of chlorides and oxygen to reach the reinforcement. Although there is general agreement that even microcracks increase the diffusion coefficient, correlation between crack width and risk of corrosion is not evident (François and Arliguie 1998, Mohammed et al. 2001). In addition to cracks, also the interfacial transition zone between cement paste and aggregates is expected to present higher diffusivity when compared to that of the bulk cement paste (Halamickova et al. 1995, Delagrave et al. 1997).

2.2 Corrosion of steel in concrete

2.2.1 Thermodynamics and pitting corrosion

Corrosion is an electrochemical process that occurs in the presence of water and oxygen and where the main redox reactions can be described by equations (2.4) and (2.5), representing the anodic oxidation of iron and the cathodic reduction of oxygen, respectively. The overall reaction is represented by equation (2.6), where the product $\text{Fe}(\text{OH})_2$, is just one of the several

possible corrosion products, depending on the surrounding environment (oxygen, pH, temperature, moisture, chloride, etc.) (Marcotte 2001).



Steel embedded in uncontaminated concrete is usually in the passive state due to the high alkalinity of the pore solution, which enables the formation of a protective iron oxide layer, i.e. passive film. The thermodynamic domains of immunity, passivity and corrosion of iron and iron oxides in solution are depicted in equilibrium potential-pH diagrams, i.e. Pourbaix diagrams (Figure 2.2) (Pourbaix 1963). The dashed lines represent the equilibrium potentials below which oxygen or hydrogen reduction occurs, according to equations (2.5) or (2.7), respectively. Between these lines, water is in equilibrium with the respective hydrolysis ions, H^+ and OH^- . Equation (2.7) is associated to environments poor in oxygen or with low pH (e.g. inside the pit) but hydrogen evolution can also occur at low potentials and in neutral to alkaline media, according to equation (2.8). At very low potentials, iron is said to be immune corresponding to a state where it is not reactive; neither does it dissolve into solution nor reacts with water to form passive oxides. At low potentials and high pH values, *low potential corrosion* may occur when the oxygen content is extremely low, possibly according to equation (2.9), although this is of no practical significance.

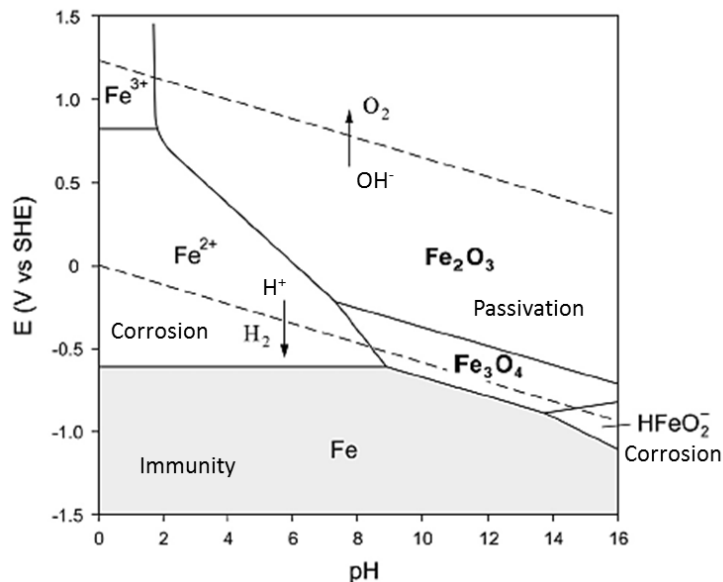


Figure 2.2. Simplified Pourbaix diagram for iron in water at 25°C (ion concentration 10^{-6} mol/l) (adapted from Angst 2011).





Figure 2.3 schematically represents the passivation of iron in aqueous solutions, in terms of current density-potential diagram. At the beginning, the anodic current rapidly increases with the potential, as iron is dissolved from the initial iron oxide free surface. As the passive film grows, the current rapidly decreases; in the passive region, iron may continue to dissolve but at a very slow rate and thus the corrosion rate is negligible. In this situation the steel is under anodic control (Bardal 2004). In the passive region, iron is covered by a very thin (1-5 nm) passive film composed of γ - Fe_2O_3 and Fe_3O_4 iron oxides, possibly formed according to reactions (2.10) and (2.11), as proposed by Alekseev (1993) and Küter (2009):



The exact composition and microstructure of the passive oxide layer formed in concrete is likely to differ from that formed in aqueous solutions since the composition of the concrete pore solution is by far chemically more complex. Moreover, along the reinforcement, variations in the composition and pH of the pore solution, oxygen gradients and presence of cement hydration products certainly condition the nature of the film. In addition, with time, a rather thick (50-200 μm) and porous layer of iron oxides interspersed with $Ca(OH)_2$ has been observed (Sandberg 1995).

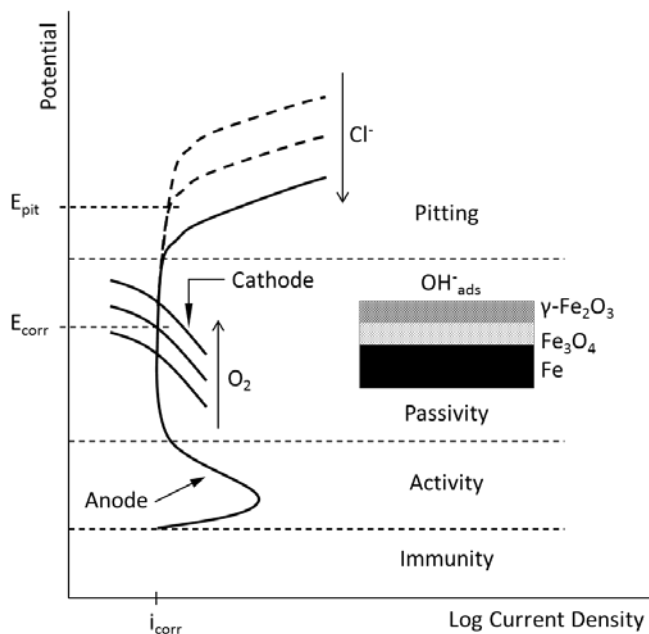


Figure 2.3. Polarization curve for steel exhibiting passivity (adapted from MacDougall and Graham 2003, Sandberg 1995). Definition of corrosion potential (E_{corr}) and pitting potential (E_{pit}). Influence of oxygen and chloride ions in E_{corr} and E_{pit} .

The corrosion potential (E_{corr}) is a mixed potential between the equilibrium potential of the anodic and cathodic reactions and depends mainly on moisture content and oxygen availability (Figure 2.3). Pitting corrosion occurs when the E_{corr} exceeds a critical potential value in the passive range of the polarization curve. This critical potential is termed pitting potential (E_{pit}) and decreases with the concentration of the aggressive species such as chloride ions (Figure 2.3) (Page and Treadaway 1982). It is worth noting that E_{pit} is not only dependent of the chloride concentration but also of other factors such as the pH of the pore solution, temperature, microstructure and composition of the concrete-steel interface or composition and surface finish of the steel (Bertolini and Radaelli 2009).

Despite vast amount of research, the role of chloride ions in pitting corrosion is not yet fully understood. Breakdown of passivity is usually ascribed to one of three main mechanisms; the penetration mechanism, the film breaking mechanism and the adsorption mechanism (Strehblow 2003 and references therein). According to the penetration mechanism, chloride ions in the electrolyte penetrate through the passive layer to the metal surface due to the high potential difference across the passive film. The film breaking mechanism, assumes that discontinuities in the passive film, such as cracks, allow direct access of chloride ions to the metal surface. Such cracks can form, for example, due to a sudden change in E_{corr} . Finally the adsorption mechanism involves the adsorption of chloride ions to the passive film leading to progressive thinning until complete dissolution. The exact mechanism leading to passive film breakdown is out of the scope of this thesis since it requires in-situ studies not possible for steel immersed in concrete. However, it is believed that the overall process of chloride induced pitting corrosion in concrete can be schematically represented by Figure 2.4.

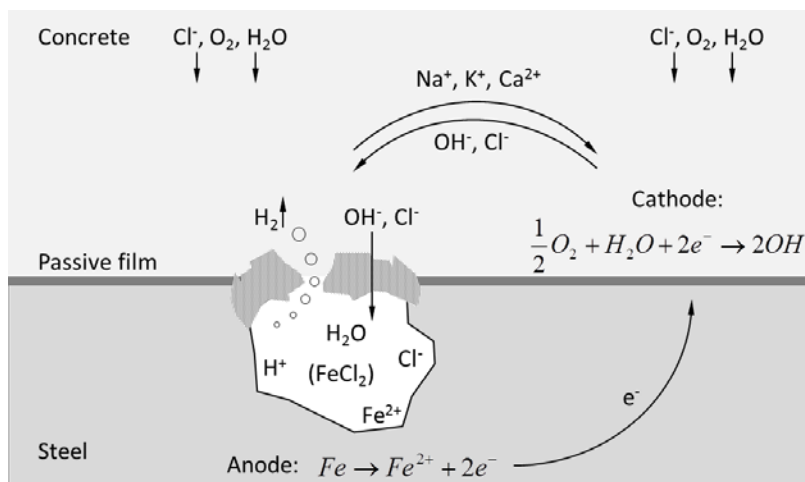
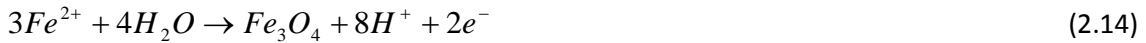


Figure 2.4. Schematic representation of chloride induced pitting corrosion.

After breakdown of passivity a pit is formed and iron dissolution proceeds according to equation (2.4). The electrons are transferred from the anode to the cathode (electronic current), where oxygen reduction takes place, according to equation (2.5) which is generally the only cathodic reaction to consider. In order to maintain electroneutrality and balance the positive charges produced at the anode, anions (OH^- , Cl^-) move away from the cathode whilst cations (Na^+ , K^+ , Ca^{2+}) move towards it, i.e. ionic current. Inside the pit, hydrolysis of dissolved iron ions takes place according to equations (2.12-2.14), causing acidification (Pourbaix 1974).

In addition, a porous cap composed of iron rust products and remnants of the passive film might be formed (Alvarez and Galvele 1984, Cheng and Luo 1999), significantly reducing the mass transport into and out of the pit. In alkaline environments hydroxyl ions will migrate into the pit to balance the formation of H^+ (equations 2.12-2.14) which could result in neutralization of the anolyte and possibly repassivation. The acid environment inside the pit is maintained by the migration of chloride ions, possibly leading to the formation of hydrochloric acid, according to equation (2.15). Given the low pH value inside the pit, cathodic hydrogen evolution can also occur according to equation (2.7) (Pickering and Frankenthal 1972); in this case, the pit acts both as anode and cathode, and as a consequence, hydrogen embrittlement of the steel may occur (Arup 1983).



Finally, several studies have reported evidence of soluble iron-chloride complexes, i.e. green rust, generally represented in Figure 2.4 as $FeCl_2$ (although other forms have been proposed) (Küter 2009 and references therein). Green rust refers to a group of iron hydroxychloride compounds, where both Fe^{2+} and Fe^{3+} as well as Cl^- ions is present, which are only stable in oxygen deprived environments. The mechanism is believed to involve the formation of these compounds at the pit, diffusion to hydroxide and oxygen richer areas and formation of solid rust products, releasing the chloride ions to further attack the passive layer. This catalytic effect is accompanied by an aggressive local acid attack, as described by equation (2.16) (Sandberg 1995), with the rust product $FeOOH$ representing one of several possible species (goethite, lepidocrocite or akaganeite) depending on the $[Cl^-]/[OH^-]$ ratio (Refait and Génin 1993).



2.2.2 Electrochemical measurement techniques

Open circuit potential and half-cell potential measurements

The corrosion potential (E_{corr}) is a relative measure of the ease of electron charge transfer between the steel and the pore solution and a property of the concrete-steel interface, not the steel itself (Hansson 1984). Measurement of E_{corr} is performed against a reference electrode, e.g. saturated calomel electrode (SCE), which can be placed either on the concrete surface above the reinforcement (in this case a wet sponge is needed for electrolytic connection) or immersed in the exposure solution (typical in laboratory setups). The reference electrode is connected to the ground terminal while the working electrode (the reinforcement) is

connected to the positive terminal of a high impedance voltmeter ($>10\text{ M}\Omega$) as shown in Figure 2.5.

In Elsener et al. (2003) guidelines for the application of the technique and interpretation of the results together with possible factors influencing the measurements are given. Among these factors, resistivity and cover depth play an important role; changes in the moisture content (e.g. by wetting the surface) shift the potential to more negative values, while the potential difference between the position above the anode and a distant cathode becomes smaller with increasing cover depth (Elsener et al. 2003). In addition also liquid junction potentials and membrane potentials have an influence in the half-cell potential measurement (Angst et al. 2009b). A number of possibilities are shown in Figure 2.5: liquid junction potentials are due to differences in the electrolyte concentration at interfaces such as between the reference electrode and the wet sponge (E_{RE-S}) or between the wet sponge and the concrete (E_{S-C}); membrane potentials are due to concentration gradients and permselective properties of the cement paste (E_C).

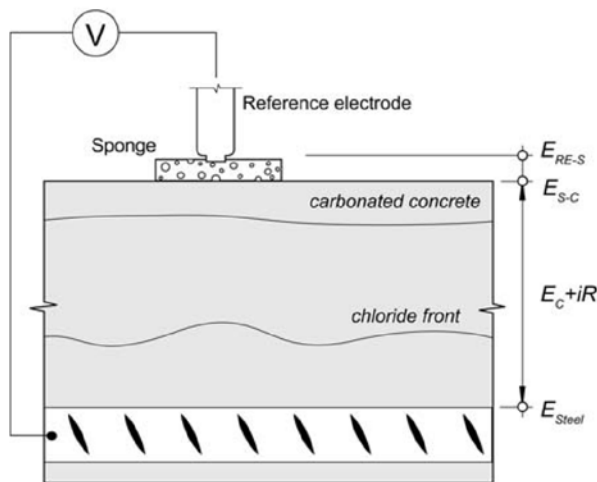


Figure 2.5. Half-cell potential measurement of steel in concrete, showing different sources of diffusion potentials (Angst et al. 2009b).

The potential difference between the working electrode and the reference electrode depends on the type of reference electrode used as well as on the passive/active state of the steel. To be able to compare between different reference electrodes, normalization is required and the potentials are normally expressed versus the standard hydrogen electrode (SHE) or versus the saturated calomel electrode (SCE), using conversion factors as exemplified in Table 2.1.

Table 2.1. Standard potentials of reference electrodes used in concrete (Vennesland 2007).

Reference Electrode	Potential (mV vs SHE)
Manganese Dioxide, MnO_2	+365
Copper/Copper Sulfate, Cu/CuSO_4	+316
Saturated Calomel	+244
Silver/Silver Chloride, Ag/AgCl	+199

Figure 2.6 schematically represents the typical range of potentials that can be found for concrete under different conditions. Typical potential values for passive steel in concrete exposed in atmospheric conditions range from -200 to 100 mV vs SCE (Bertolini et al. 2004).

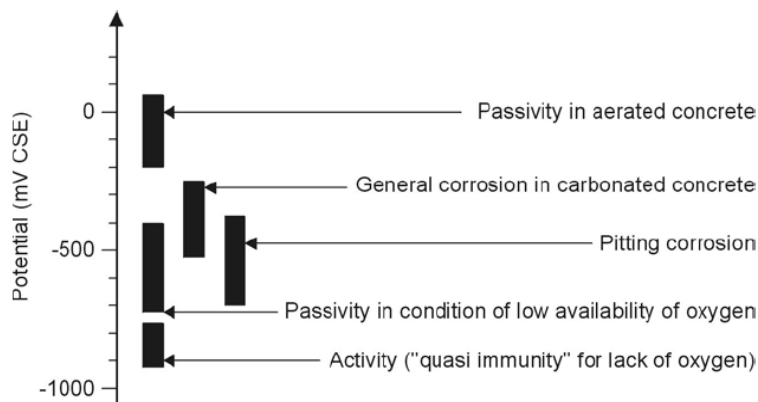


Figure 2.6. Typical range of potentials of steel in concrete (Bertolini 2004).

Potentiostatic measurements

In potentiostatic control experiments, the steel bar is kept under anodic polarisation and the corrosion activity of the steel electrode is monitored by measuring the current passing from the working electrode to a counter electrode, in order to maintain E_{corr} at a constant level by means of a potentiostat. The counter electrode is either embedded in the specimen (Arup and Sørensen 1995, Sandberg 1998) or immersed in the exposure solution (Alonso et al. 2002, Nygaard and Geiker 2005), as schematically represented in Figure 2.7. Under potentiostatic conditions, depassivation is marked by an abrupt increase in the current.

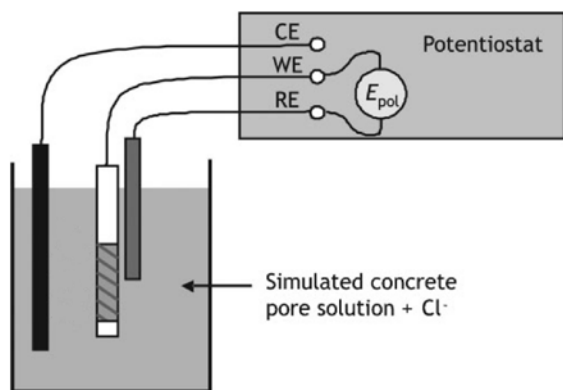


Figure 2.7. Experimental arrangement for potentiostatic measurements on steel immersed in chloride solution (adapted from Bertolini and Radaelli 2009).

One of the major discussion issues around this method is the fact that because the imposed polarisation shifts the steel potential away from its natural E_{corr} , it can influence both the characteristics of the passive film and the chloride threshold value. According to a literature review by Alonso and Sanchez (2009), the potentiostatic control method usually gives lower chloride threshold values as well as narrow scatter when compared to natural methods (open circuit conditions). Although there exists no consensus regarding the fixed potential, values

more positive than -250 mV vs SCE are usual, since in this range of potentials, the chloride threshold value is not affected by the polarisation and the type of passive layer does not vary significantly (Alonso and Sanchez 2009 and references therein). However, it is still not clear why the critical chloride content is lower. A possible explanation could be that under potentiostatic control, repassivation of incipient pits is more difficult and thus stable pit growth is achieved earlier. An observation supporting this is the fact that in the study by Nygaard and Geiker (2005) under potentiostatic controlled conditions, clear visible pits were found in only a few hours after depassivation while in the study by Angst et al. (2011a) under free corrosion conditions, days or even weeks were required to produce pits of similar size. Contrary to these observations are the results from Sandberg (1998) where even under potentiostatic control, activation-repassivation events were observable. Moreover, it should be mentioned that in the present work, under open circuit conditions, clear pits were observed in only a few hours after the first signs of depassivation (Paper V). Therefore, other factors may contribute to the lower critical chloride contents often reported for tests under potentiostatic control, such as the influence of the polarization current in the chloride ingress and the relationship between the chloride content at the interface and that measured in samples from the bulk concrete.

2.2.3 Electrochemical rehabilitation methods

Electrochemical methods aim to guarantee or extend the service life of reinforced concrete structures by thermodynamically reversing the effects usually caused by aggressive species. There are three main methods: cathodic protection (CP), electrochemical chloride extraction (ECE) and electrochemical realkalization (ER). All methods share the same principle: the polarisation of the steel reinforcement by (permanent or intermittent) application of cathodic current (Figure 2.8). However, the duration of the treatment and the current density applied is different depending on the method (Table 2.2) and degree of contamination.

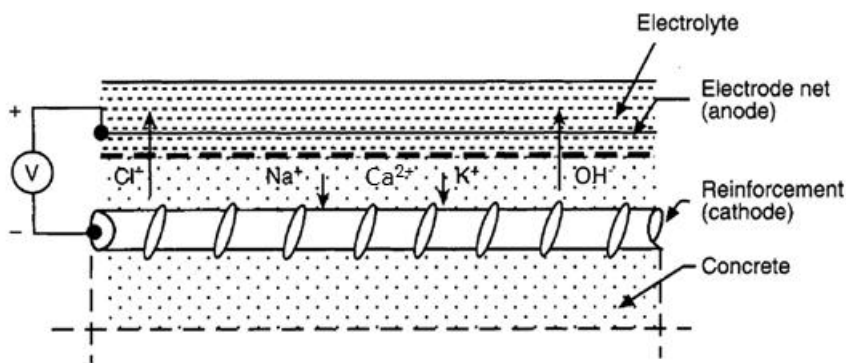


Figure 2.8. Principle of electrochemical rehabilitation methods (adapted from Mietz 1998).

Table 2.2. Characteristics of electrochemical rehabilitation techniques (Mietz 1998).

Method	CP	ECE	ER
Current density (mA/m ²)	3-20	800-2000	800-2000
Duration of treatment	Permanent	6-10 weeks	3-14 days

The consequences of the cathodic polarisation of steel are three fold: (1) the corrosion potential is lowered to values below the pitting potential, thus allowing for repassivation of the reinforcement even in chloride containing environments; (2) the alkalinity at the steel increases due to the cathodic oxygen reduction; given the higher availability of OH^- in the vicinity of the steel, local pH decrease in the case of pitting corrosion may be avoided and (3) migration of cations (Na^+ , K^+ , Ca^{2+}) to the cathode and anions (OH^- , Cl^-) to the anode reducing the chloride concentration at the steel surface. On the other hand, electrochemical methods may also present side-effects namely: (1) alkali-silica reaction in the case of reactive aggregates due to the higher concentration of OH^- in the pore solution; (2) hydrogen embrittlement of the steel due to the reduction of water at very negative potentials and (3) loss of adhesion between steel and concrete presumably due to increased porosity (Mietz 1998, Polder 2003).

Cathodic prevention (CPre) was first introduced by Pedferri (1992). It can be seen as a type of CP intended for new structures where chloride ingress is expected. The principle is the same as that of other electrochemical methods mentioned before, although lower current densities are applied, typically $1\text{-}2 \text{ mA/m}^2$ (Bertolini et al. 2004). The effect of CP and CPre in the chloride threshold value is illustrated in Figure 2.9. At the beginning of the exposure the steel is in the passive state (point 1). As the chloride concentration increases the pitting potential (E_{pit}) decreases. When the critical chloride content is reached, depassivation takes place (point 4). At this point, if the reinforcement is polarized by the application of cathodic current (as in CP), E_{corr} drops to more negative values (points 5 or 6) where corrosion ceases. If instead, current is impressed at the beginning of the exposure (CPre), the initial E_{corr} is significantly lower (point 2) and thus the critical chloride content for pitting corrosion is now much higher (beyond point 3) (Bertolini et al. 2009 and references therein). Cathodic current can also be applied to concrete, for only a short period previously to exposure, after curing or even in the fresh state. In Buenfeld et al. (2004), the electrochemical treatment consisted in the application of a current density of 4 A/m^2 of steel during 10 days; for a comparable interfacial air void content, the results indicated a marked increase in the C_{th} to levels higher than 2% whereas in non-treated samples this value was approximately 0.5%.

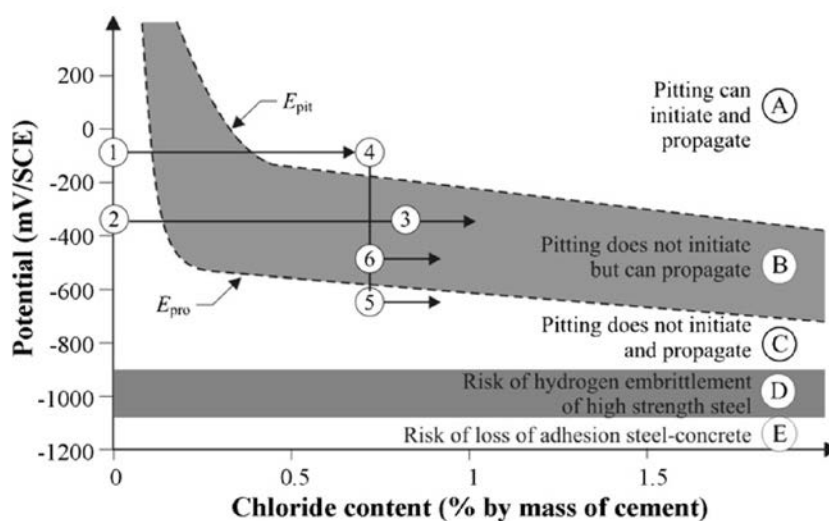


Figure 2.9. Steel potential versus chloride content in concrete (in Bertolini et al. 2009).

2.3 Corrosion initiation and chloride threshold values

Studies of chloride induced corrosion initiation of steel in concrete are quite often associated with the determination of chloride threshold values (C_{th}), given the importance of this parameter in service life design of reinforced concrete structures. Two definitions of C_{th} are common; under a scientific point of view, C_{th} is defined as the chloride content required for depassivation of steel whilst under an engineering point, C_{th} is usually the chloride content associated with visible or acceptable deterioration (Angst et al. of 2009a). The first definition suites better the scope of the present thesis.

Corrosion initiation and C_{th} are affected by a number of factors; concrete-steel interface pH of the pore solution, steel potential, binder type, surface condition of the steel, moisture content, oxygen availability, water-binder ratio, resistivity, degree of hydration, type of steel, temperature, chloride source, cation accompanying the chloride ion, inhibitors and electrochemical treatment (Angst et al. 2009a). This section gives an overview of the influence of some of these factors in the resistance to chloride induced corrosion. Within the scope of this thesis these are: the steel surface condition; the concrete-steel interface and the binder type and pH of the pore solution.

2.3.1 Surface condition of the steel

In essence, corrosion is a metallurgical problem. Thus, for research purposes, steel in the “as-received” condition cannot be considered as representative or reproducible (Page 2009). On the other hand, the use of smooth bars or pre-treatments, such as polishing or sandblasting, is not representative of the conditions in the practice (Angst et al. 2009a). As such, the surface condition of the steel plays an important role on the depassivation process, not only in terms of its intrinsic resistance (e.g. composition and uniformity of the mill scale) to chloride induced corrosion but also because it influences the microstructure characteristics of the interface with the concrete. Horne et al. (2007) reported higher levels of portlandite at the interface of wire-brush clean bars at late ages, when compared to uncleaned bars.

The corrosion resistance of a metal depends on the amount of impurities (e.g. inclusions), defects in the mill scale (e.g. cracks or crevices) or lattice imperfections. Due to these compositional variations anodic and cathodic sites may be generated at the steel surface. Such differences cause some sites to be more electrochemically active than others and thus generating potential gradients. In carbon steel this can happen between the ferrite and the iron carbide phase, where the ferrite phase tends to develop a more active potential than the iron carbide. Potential gradients are also likely to develop in regions of uniform composition since the atoms at the grain boundaries tend to be more active (anodic) than the atoms in the bulk (Küter 2009). In addition, the anodic and cathodic reactions in the passive state may give rise to localized concentration differences (Cl^- , OH^- , H^+) along the concrete-steel interface which can lead to the formation of more electrochemically active sites.

Evidence of this electrochemical inhomogeneity leading to preferential adsorption of chlorides is given in e.g. Lin et al. (2010) while studying steel in solutions: by simultaneously mapping the

corrosion potential and chloride concentration at the steel surface, the authors found that MnS inclusions were preferential sites for Cl^- ion accumulation due to the generation of potential gradients. In a study by Pillai and Trejo (2005) microscopic investigations revealed that after removal of the mill-scale, a large number of sulphide inclusions had been exposed and that these acted as corrosion initiation sites. The pitting susceptibility of MnS inclusions in chloride environments is attributed to the preferential adsorption of chloride ions at these sites, resulting in their electrochemical dissolution when the steel is at a resting potential (Webb et al. 2001).

In addition to inclusions, the mill-scale also plays a significant role in the resistance to chloride induced corrosion: on the one hand, crevices seem to act as preferential nucleation sites (Li and Sagues 2001, Pillai and Trejo 2005, Ghods et al. 2011), while on the other hand, a porous mill-scale may allow the ingress of ions from the concrete and possibly delay the corrosion onset (Jaffer and Hansson 2009). Mahallati and Saremi (2005) found that the presence of mill-scale caused a decrease in the electrical resistance of the passive film; the mill-scale acted as a barrier impeding O^{2-} and OH^- to reach the bare metal surface and hence significantly delaying the passivation even in high alkalinity solutions. Pillai and Trejo (2005) compared the behaviour of as-received and polished surfaces for different types of steel and found that higher chloride thresholds could be obtained by removing the mill-scale. This effect was attributed to the presence of crevices in the mill-scale which could lead to the formation of microgalvanic cells between areas covered with mill-scale and areas without it. Ghods et al. (2011) observed that cracks in the mill-scale linking voids and crevices to the bare steel surface served as preferential routes for concrete pore solution ions to penetrate and reach the free steel surface. A mechanism similar to that of crevice corrosion was suggested; oxygen depletion in the crevice resulted in reduced OH^- concentration leading chlorides to migrate into the crevice to maintain electroneutrality.

Finally, stresses can also induce significant inhomogeneities along the steel surface, leading to local potential differences; strained regions are usually more electrochemically active than unstrained metal surfaces; the former thus behaves anodically while the later cathodically (Bentur et al. 1997).

2.3.2 Concrete-steel interface

Steel cast in concrete is usually more resistant to chloride induced corrosion than when immersed in alkaline solutions, however, the micro and macrostructure and the composition of the interface, can significantly affect the resistance of the reinforcement to corrosion initiation and consequently C_{th} . As careful as mix design, execution and curing may be defects at the interface will always exist; gaps are formed due to settlement and collection of bleeding water under horizontal reinforcement while entrapped air voids may be associated to the mix design and compaction procedures. The importance is such that according to Yonezawa et al. (1988), air voids at the interface were considered essential for corrosion initiation, whereas Mohammed and Hamada (2001) defined C_{th} as the “chloride ion concentration that caused the initiation of active corrosion of steel bars in concrete, provided that there are no voids/damages at the steel-concrete interface”.

The main corrosion inhibiting characteristics of the concrete-steel interface are attributed to the presence of a segregated calcium hydroxide layer at the steel surface (Page 1975, Al Khalaf and Page 1979, Monteiro et al. 1985). This layer physically limits the access of oxygen and chlorides to the steel surface and facilitates repassivation by restricting the tendency for a decrease in the local pH due to consumption of OH⁻ in the anodic reactions within incipient pits at the metal surface (Page and Treadaway 1982, Yonezawa et al. 1988).

Given that the interface microstructure depends on the casting direction, it is not surprising that the underside of horizontal cast steel bars shows higher porosity (Horne et al. 2007) and that this region is more susceptible to pitting corrosion. In a study by Angst et al. (2011b), it was even observed that corrosion initiated on the underside of the rebars with respect to casting direction, regardless of the direction of the chloride penetration. The importance of entrapped air voids and gaps in the corrosion initiation has been demonstrated in a number of studies (Sandberg 1998, Arliguie et al. 2003, Söylev and François 2003, Hartt and Nam 2008, Ryou and Ann 2008, Zhang et al. 2011). However, very little quantitative information that correlates the amount and size of air voids with C_{th} is available. This is due to the difficulty in measuring air void content at the interface non-destructively (Ann and Song 2007). Figure 2.10 shows one of the few available correlations in the literature to quantitatively report the dependency of C_{th} with the amount of interfacial air voids. Similar data is provided in (Buenfeld et al. 2004), according to which, the C_{th} significantly increases when the interfacial air void content is reduced to less than 0.8%.

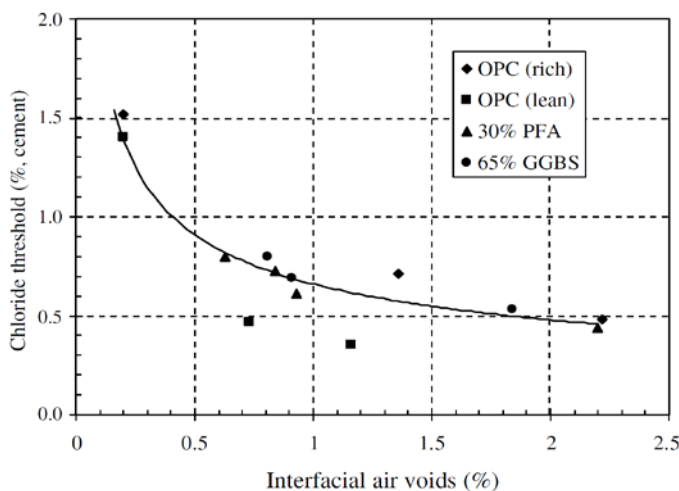


Figure 2.10. Chloride threshold as function of interfacial voids (in Ann and Song 2007).

A possible consequence of air voids is the formation of potential gradients on the surface of the steel due to differences in the microenvironment surrounding the steel (oxygen and moisture content, aggressive species, pH). Areas of the steel surface within the air void have higher access to oxygen and thus tend to become more cathodic whilst regions protected by adherent cement hydration products tend to become anodic (Küter 2009). Under saturated conditions, air voids provide a more active environment for electrochemical reactions than the dense cement matrix that can relatively restrict the current flow between anode and cathode (Ann and Song 2007).

Finally, there is also a need for quantitative studies aiming to correlate the chloride content measured in the bulk concrete by traditional sampling methods with that at the location where corrosion actually occurs, i.e. at the interface. In this regard it has been demonstrated that the chloride content along the reinforcement can be as twice as high as that at the same depth away from the rebar due to reinforcement obstruction effect and spatial distribution of coarse aggregates (Yu and Hartt 2007, Yu et al. 2007, Hartt and Nam 2008). In addition, non-uniform chloride distributions along the interface have been reported as well as higher chloride contents in the vicinity of anodic regions when compared regions of the interface in the passive state (Yu et al. 2010).

2.3.3 Pore solution and binder type

The stability of the passive film increases with the pH (Verink and Pourbaix 1971). Portland cement concrete pore solution is mainly composed by saturated calcium hydroxide (pH 12.5) with and small quantities of other alkalis (Na^+ , K^+) that raise the pH to levels around 13.5. The pH of the pore solution depends on the cement alkalinity and binder type; when blended cements are used, a reduction on the pH is expected (Byfors 1987). Also Cheng et al. (2005) reported pH values for GGBS concrete in the order of 12.4-12.8. In this range of pH's it has been demonstrated that steel behaves different than it does when the pH is above 13 (Veleva et al. 2002). It is however not fully understood how the composition of the pore solution affects the quality of the protective oxide, in particular the influence of the sulphate ions (from the gypsum in the cement) in the development of the passive film (Ghods et al. 2009) or the role of sodium and potassium in the corrosion process (Poursaee and Hansson 2009). Montemor et al. (1998) showed that the presence of fly ash led to an increase in the amount of iron oxyhydroxide (FeOOH) in outer layers of the film and to an increase in the thickness of the passive film. Gui and Devine (1994) investigated passive films formed on iron in alkaline solutions containing sulfates and demonstrated that the structure and nature of the passive oxides was affected by the adsorption of the sulphate ions. Similar conclusions have been reported by Ghods et al. (2009).

In addition to the effect on the pH, the type of binder influences the corrosion resistance by altering the chloride binding capacity. Chemical binding can be improved by the addition of fly ash and slag because these mineral additives form additional calcium aluminate hydrates whereas the opposite is valid for silica fume (Justnes 1998). On the other hand, mineral additions improve physical binding by contributing to the formation of CSH gel thus providing more surface area for chloride adsorption. With regard to C_{th} the available data is somewhat contradictory, as reviewed by Angst et al. (2009a); while on the one hand improved chloride binding capacity may contribute to an increase in C_{th} , on the other hand, the expected decrease in the pH of the pore solution contributes for the instability of the passive film. Finally, the effect of the secondary pozzolanic reactions in the microstructure of the concrete-steel interface should also be taken in consideration, in particular with regard to the concrete resistivity, expected to increase, which in turn will have an impact on the ionic current flow.

2.4 Chloride content measurement

2.4.1 Current practice and techniques

The ability to measure chloride in cementitious materials is of great importance due to the significance of chloride-induced corrosion affecting reinforced concrete structures. The determination of the chloride content in concrete is well documented in standards (EN196-21 1989, AASHTO-T260 1997) and technical documents (Andrade and Castellote 2002). Typically, measurement involves the extraction of chlorides from powder samples with nitric acid followed by quantification by Volhard titration, potentiometric titration using ion selective electrodes or spectrophotometric methods. Nevertheless several laboratories have developed their own protocols and a number of different extraction and quantification procedures have been proposed (Chaussadent and Arliguie 1999, Climent et al. 1999, Potgieter et al. 2004, Potgieter and Marjanovic 2007). X-ray fluorescence spectrometry (XRF) can be used for measurement of the total chloride content, significantly reducing sample preparation and time of analysis (Dhir et al. 1990, Proverbio and Carassiti 1997). This is particularly interesting for routine analysis such as in the case of cement production.

The two most common concrete sampling techniques for chloride analysis are core drilling and dust collection from borehole dry drilling. Concrete cores are either depth grinded or cut into slices, which are crushed, powdered and homogenised for further chloride analysis. Although grinding methods may allow depth steps down to 0.5 mm, the chloride profiles spatial resolution is usually in the range of a few millimetres and thus care should be taken during the slicing/grinding procedure to account for a representative sample at the depth of the reinforcement. On the other hand, the analysis of powder samples collected by borehole dry drilling has shown large variations and two main error sources have been identified: accuracy of the depth at which the sample is taken and contamination of the samples by powder transport from previous sampling depths, leading to overestimation of the chloride content at each depth (Wall and Nilsson 2008). Moreover, for both sampling methods, the core/bore diameter should be carefully selected as a function of the maximum aggregate size, so as to minimize its influence in the measurement (Nilsson et al. 1996, de Rooij and Polder 2005).

High spatial resolution scanning techniques are therefore advantageous for studies of chloride ingress in concrete, enabling continuous profiling, while reducing sample preparation and time of analysis. In this regard, a number of techniques have been successfully employed. Wilsch et al. (2005) demonstrated the applicability of laser-induced breakdown spectroscopy (LIBS) for surface scanning and depth profiling of chlorides in concrete within a resolution range of 2 mm and a limit of detection of 0.15 wt% of cement. Ban et al. (2011) proposed the application of near-infrared (NIR) spectrometry for in-situ measurement of the chloride content and found a good correlation with measurements by classical chemical titration. Limits of detection of 0.05 wt% of cement were reported by Burakov et al. (2007) applying a combination of laser/electrospark laser spectroscopy in cement pastes. Finally, a number of researchers (Jensen et al. 1996, Jensen et al. 1999, Win et al. 2004, Wall and Nilsson 2008) have used electron probe micro analyser (EPMA) to study 2D chloride distributions, diffusion coefficients

and penetration profiles in cracked concrete. Limits of detection as low as 0.005 wt% of cement, with a spatial resolution of 100 μm have been reported (Mori et al. 2006).

2.4.2 LA-ICP-MS innovative approach

Laser ablation inductively coupled plasma mass spectrometry (LA-ICP-MS) is a suitable technique for the characterization of solid samples in materials science, enabling multi-element spatial identification and quantification at very low concentration levels (ppm range or below) and at a submicron-scale (Gunther and Hattendorf 2005). The technique can be divided into two main components; the laser ablation system and the ICP-MS. A brief description of the operating principles behind both techniques is given below. LA-ICP-MS is schematically represented in Figure 2.11.

In laser ablation, a laser beam is focused directly to the surface of the sample. A pulse of energy from the laser ablates a fixed quantity of material, which depends on the energy of the laser beam, the power applied, the laser repetition rate or duration of the pulse and the melting point and volatility of the sample material (Russo et al. 1998). A solid aerosol is created which is then transported by an inert gas (argon or helium) to the plasma for atomization and ionization. As the analyte enters the plasma and ions are formed, the magnitude of the signal increases to a maximum and then gradually tails off to the background as the analyte is depleted. Spatial resolution of the sample under analyses depends on the wavelength of the laser and the optics used to focus it on the specimen. Detection limits are directly related to the amount of material ablated from the sample. Typical limits obtained from a 25 μm diameter crater are in the 0.1-10 $\mu\text{g/g}$ range (Taylor 2001). Detection limits can be improved by optimizing the flow rates of the carrier gas and the energy characteristics of the laser for various sample matrices.

To calibrate LA-ICP-MS, standard reference materials or laboratory-produced matrix-matched samples are employed. However, fluctuations in the laser energy or differences between the ablated volume in the reference and in the sample can occur. In order to improve the robustness of the calibration, an internal standard can be used. This is usually a homogeneously distributed and naturally occurring element of known quantity both in the reference material and in the sample (Ito et al. 2009).

As mentioned previously, the analyte elements are atomized and ionized in the plasma where the ion composition is proportional to the concentration of the analyte species in the original sample. The ions are then representatively sampled and extracted from the plasma (ICP in Figure 2.11) at the interface facilitating their transport into the mass spectrometer. Under the influence of an electromagnetic field, the quadropole mass spectrometer aligns the ions of interest with the detector, deflecting the remaining ones.

In concrete technology, LA-ICP-MS applications include the analysis of radioactive isotopes (Gastel et al. 1997), studies on the durability of FRP reinforcements (Dejke 2001) and the investigation of the protection mechanism of lithium nitrate against alkali silica reaction (Feng et al. 2010). The determination of chlorides in sediment samples has been proposed by

Boulyga and Heumann (2005), using isotope dilution LA-ICP-MS, with significant good results (detection limits of 8 $\mu\text{g/g}$).

Given the expected variability in the microenvironment along the concrete-steel interface, the use of highly spatial resolved scanning techniques for chloride determination is advantageous enabling continuous profiling, while reducing sample preparation and time of analysis. However, measurement of chloride in cementitious materials is a very challenging task because of the high heterogeneity of the concrete. Matrix-matched reference samples are required but difficult to produce and aggregate discrimination should be taken in consideration as the chlorides are present (bound or free) in the cement paste.

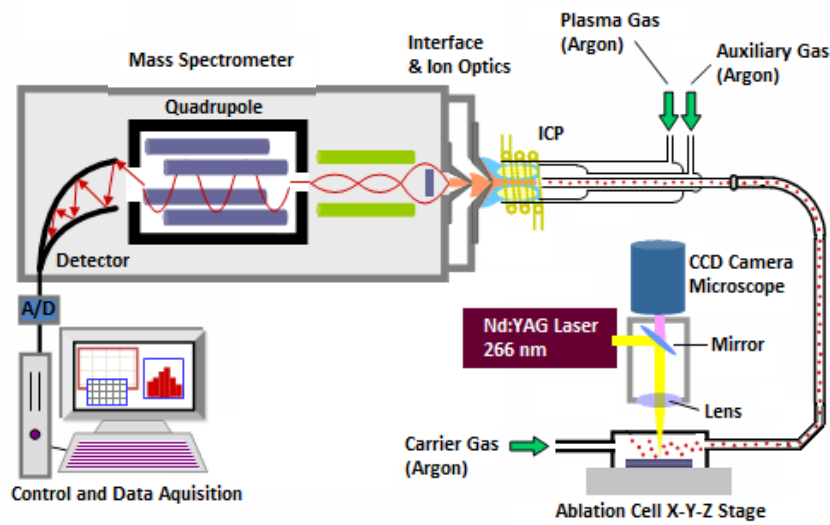


Figure 2.11. Schematics of LA-ICP-MS technique (Paper I).

3 Experimental Work

This chapter describes the experimental work in this thesis, which was divided in three main parts. The first (Section 3.1) deals with the development of a method for space resolved analysis of chlorine, and other elements, in cementitious materials by means of LA-ICP-MS; the main results are summarised in Paper I. In the second part (Section 3.2) of the experimental work, the chloride distributions along the concrete-steel interface were studied according to the methodology proposed previously. The main purpose was to evaluate possible differences along the interface while the steel was in the passive state and later, after corrosion initiation, between passive and active regions. This work was supplemented with SEM-EDS microstructural studies mainly at anodic locations and XRD analysis of corrosion products. The main results from the second part are presented in Papers II, III and IV. Owing the limitations of the second part with regard to the representativeness of data at the time of depassivation, the third part of the work, aimed at verifying the chloride distributions along the interface at the very first signs of depassivation. In addition, the influence of different cement replacing materials and electrochemical treatment of the concrete cover in the C_{th} were studied. The main results from this section are presented in Paper V.

3.1 LA-ICP-MS method development

3.1.1 Reference materials

Calibration of LA-ICP-MS is usually performed using standard reference materials (SRM); however, given the difficulty in finding suitable SRM for concrete, laboratory reference samples were prepared for this study. Whenever semi-quantitative measurements were carried (Papers I to IV), optimization of the analytical settings and calibration of the LA-ICP-MS was based on Portland cement concrete powder pellets as reference material (OPC1 in Table 3.1). For cross checking of the calibration and assessment of the influence of the sample matrix in the chloride detection, measurements were done on concrete powder pellets made from different cement types (Paper I). In Table 3.1, the chloride concentration in the different pellets, determined by potentiometric titration (AASHTO-T260 1997), is presented. The range of concentrations was chosen based on the restrictions imposed by EN 206-1 (2000) and the range of C_{th} values reviewed by Angst et al. (2009b). Detailed preparation of the pellets is given in Paper I. Furthermore, other materials were used in this part of the work; chloride ingress profiles after the diffusion and migration tests were qualitatively assessed in cement paste, mortar and concrete samples.

Table 3.1. Chloride concentrations in the pellets used for optimization and calibration (Paper I).

	Cl content (wt% of sample)				
OPC1 (CEM I)	0.036	0.076	0.115	0.223	0.332
OPC2 (CEM I)	0.022	0.042	0.063	0.174	0.285
GGBS (CEM III/B)	0.017	0.032	0.047	0.127	0.210
FA (CEM II/B-V)	0.017	0.033	0.047	0.127	0.208

3.1.2 Operating conditions

The general set-up and operating principle of the LA-ICP-MS system was described previously in section 2.4.2. The equipment used in this project was a CETAC LSX-200 laser ablation system coupled to a Perkin Elmer Sciex Elan 6000 quadrupole ICP-MS. The LSX-200 is equipped with a large sample cell with internal dimensions of 10.4 cm x 7.9 cm x 5.9 cm (length x width x height) and a volume of 482 cm³ (Carugati et al. 2010). Instrumental settings were optimised based on chloride ion signal intensity and spatial resolution and are presented in Table 3.2. The recorded isotopes were ³⁵Cl, ⁴⁴Ca and ⁵⁶Fe.

Table 3.2. Instrument operating conditions and experimental parameters of the LA-ICP-MS.

Elan 6000 ICP-MS		CETAC LSX-200	
RF Power (W)	1250	Laser Source	Nd:YAG
Dwell Time (ms)	50	Wavelength (nm)	266
Sweeps	6	Pulse Width (ns)	< 6
Carrier gas flow rate (l/min)	0.85	Spot Size (µm)	300
Recorded Isotopes	³⁵ Cl, ⁴⁴ Ca, ⁵⁶ Fe	Pulse Energy (mJ/pulse)	7.5
		Repetition Rate (Hz)	20
		Scan Rate (µm/s)	100

3.2 Chloride distributions and steel surface conditions

3.2.1 Materials

The mixture proportions and geometry of the concrete specimens used in this part of the project is given in Table 3.3 and Figure 3.1, respectively. In each specimen, eight smooth cool-drawn carbon steel bars were cast at four different cover depths; 10, 15, 20 and 25 mm. Three types of steel surface condition, as shown in Figure 3.2, were tested; special delivered (SD), as-received (AR) and chemically cleaned (CC). A total of four specimens were produced; SD1, SD2, AR and CC. All SD type steel bars in series B were studied under potentiostatic control (0 mV vs SCE) according to Nygaard and Geiker (2005). The remaining steel bars were kept under open circuit. Reference to the specific steel bar(s) under study is given in each paper (Papers II to IV). A detailed description about the materials used, specimen preparation and pre-conditioning and electrochemical monitoring techniques used is given by Boubitsas and Tang (2012) and in Paper IV.

Table 3.3. Concrete mixture proportions (Paper I).

CEM I 42.5 N (kg/m ³)	Aggregates 0-10 (kg/m ³)	Water (kg/m ³)	Superplasticiser (wt% CEM)	Slump (mm)	Air (%)	Compressive Strength at 28 days (MPa)
380	1817	190	0.5	180	3	58

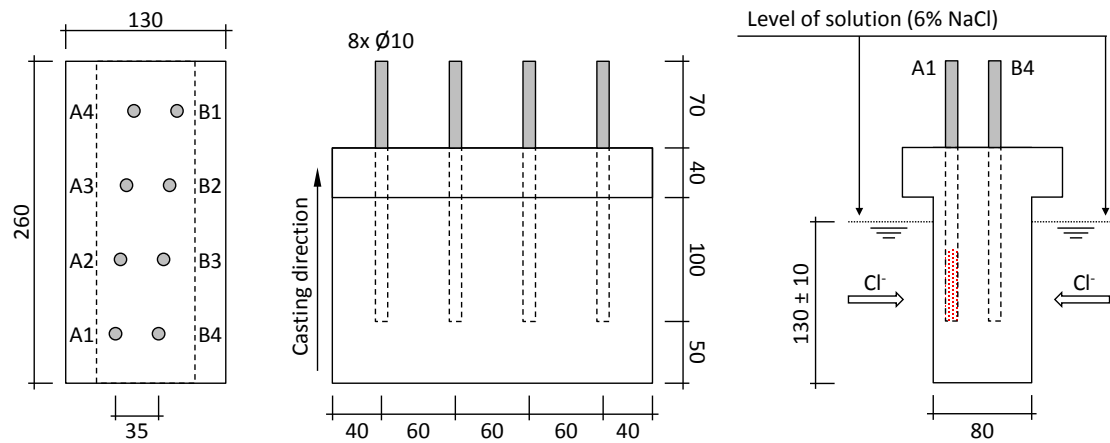


Figure 3.1. Geometry of the test specimen (dimensions in mm). Corrosion usually started within the area marked in red (adapted from Boubitsas and Tang 2012) (Paper I).

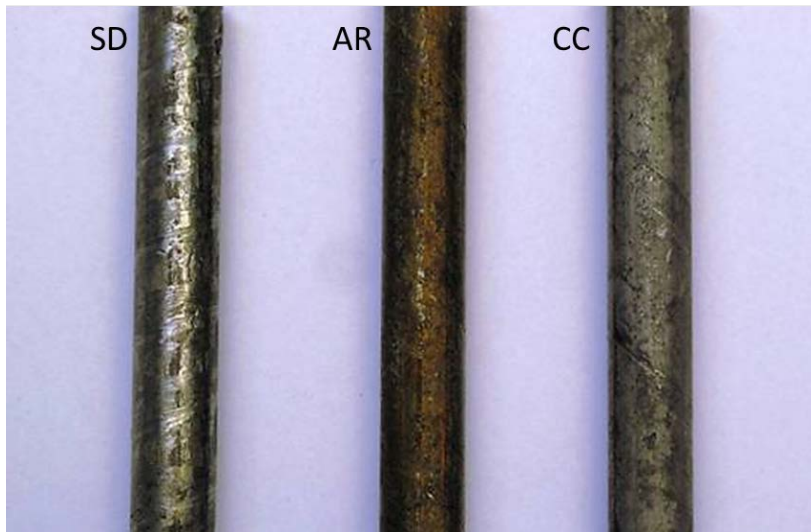


Figure 3.2. General aspect of the three types of steel surfaces studied (Boubitsas and Tang 2012).

3.2.2 Methods

Visual inspection

As a routine inspection, after the corrosion monitoring the embedded steel bars were released from concrete specimens by cutting grooves near the steel bar and splitting. The concrete-steel interfaces (both on the concrete and the steel bar surfaces) were visually examined for possible defects and corrosion spots. The surface conditions were photographed by an ordinary digital camera.

Optical microscopy

For some selected samples (Paper II), visual inspection was supplemented by means of high resolution digital photography under an optical microscopy. In this case the section of the interface were first mounted on a glass slide with a UV-light curing adhesive, followed by impregnation, under vacuum, with epoxy resin containing fluorescent dye. After hardening,

the pieces were lapped and polished on a rotary polishing machine equipped with a metal bound 30 µm diamond grinding wheel. Generally 200 µm grinding steps, against the direction of the chloride penetration front, were performed and photographs were taken at each step, both under white and UV light.

LA-ICP-MS

The meso-scale chloride, calcium and iron distributions along the concrete-steel interface were studied by means of LA-ICP-MS, according to section 3.1.2. The portion of a specimen of interest was cut, using a fine diamond saw with limited flow of cooling water, to a size suitable for mounting in the scanning chamber. No special sample preparation was required. Previous to the analysis of each sample, the technique was calibrated according to section 3.1.1.

Scanning electron microscopy (SEM)

For some selected samples (Paper II and IV), scanning electron microscopy (SEM) was employed to supplement LA-ICP-MS with qualitative X-ray microanalysis of the concrete-steel interface, in particular around the active corrosion sites. A JEOL JSM-5310LV operated in the backscattered electron mode (BSE) was coupled with an energy dispersive spectroscopy (EDS) detector (Oxford Instruments) for element mapping.

X-ray diffraction (XRD)

For some selected samples (Paper II and IV), corrosion products were collected from the concrete-steel interface and analysed by X-ray diffraction (XRD). Together with the microstructural information from SEM-EDS, a better insight on the distribution of these rust products around the pits is possible. In this study a Siemens D5000 powder diffractometer was used.

3.3 Chloride distributions at the time of depassivation

Further details regarding the experiments in this part of the work are given in Paper V. Most of the experimental procedures followed the recommendations of the RILEM TC 235 CTC draft proposal for a test method for chloride threshold value in concrete (2011).

3.3.1 Materials

In this part of the work six concrete compositions were studied; the mixture proportions and geometry of the test specimens is given in Table 3.4 and Figure 3.3, respectively. For each mix, four specimens were prepared and two of them were electrochemically treated (according to section 3.3.2) prior to pre-conditioning.

Table 3.4. Concrete mixture proportions (Paper V).

Batch	Binder Type	w/b^2	Binder (kg/m ³)	Water (kg/m ³)	Aggregates (kg/m ³)	Superplasticizer (wt% binder)	Slump/Spread (mm)	Compressive Strength at 28d (MPa)
ANL055	100%PC ¹	0.55	348	191	1802	0.70	95/-	42.0
ANL045	100%PC	0.45	393	177	1802	1.69	75/-	56.8
SCC ³	60% PC + 40% FA	0.52	350 + 140	202	1541	2.16	-/680	43.1
FA055	70% PC + 30% FA	0.55	284 + 85	170	1802	3.18	150/-	64.5
GGBS055	70% PC + 30% GGBS	0.55	265 + 80	190	1802	1.10	165/-	36.4
SF055	95% PC + 5% SF	0.55	319 + 16	193	1802	1.54	125/-	42.4

¹PC refers to Swedish Portland cement for civil engineering, corresponding to CEM I 42.5N BV/SR/LA.

²Considering the activity coefficients 0.3, 1 and 2 for pozzolanic additions of FA (fly ash), GGBS (ground-granulated blast-furnace slag) and SF (silica fume), respectively.

³SCC refers to self-compacting concrete.

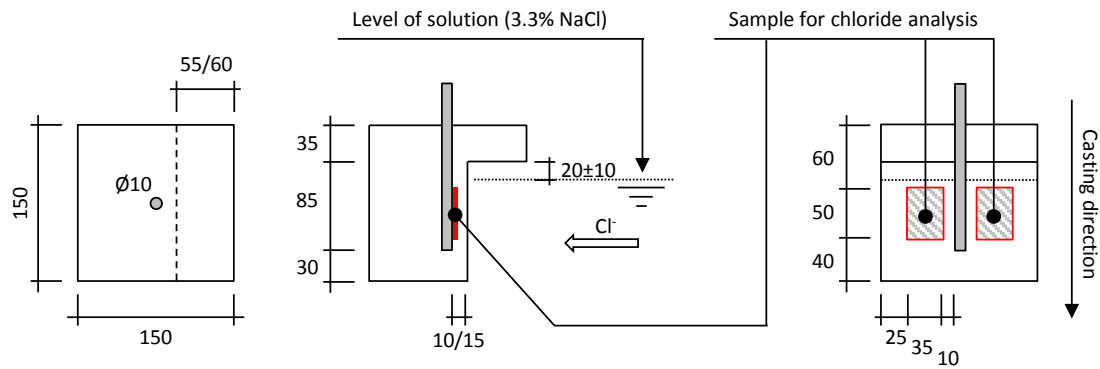


Figure 3.3. Geometry of the test specimen (dimensions in mm) (Paper V).

In each specimen, one smooth cool-drawn carbon steel bar was embedded. Prior to casting, the steel bars were clean in acid and pre-rusted (Figure 3.4).

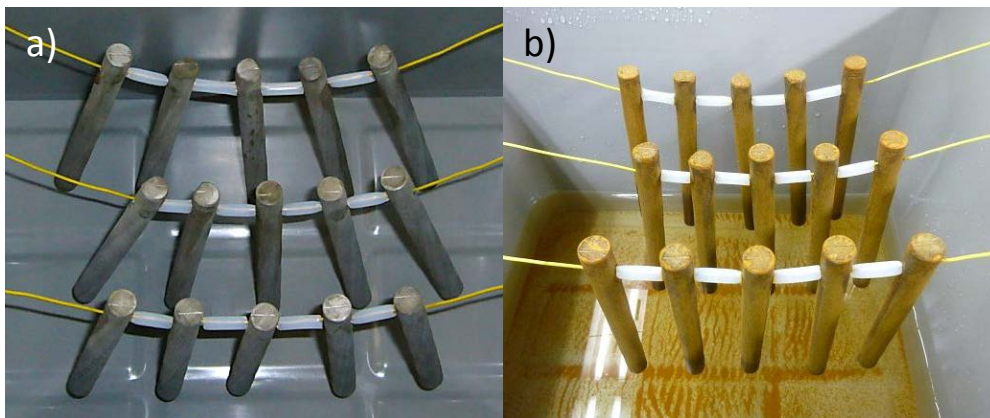


Figure 3.4. General aspect of the steel bars (a) after acid cleaning and (b) after pre-rusting.

In order to guarantee the correct positioning of the steel bar in the specimen, a special plywood insert was design and fit into the mould, as shown in Figure 3.5.

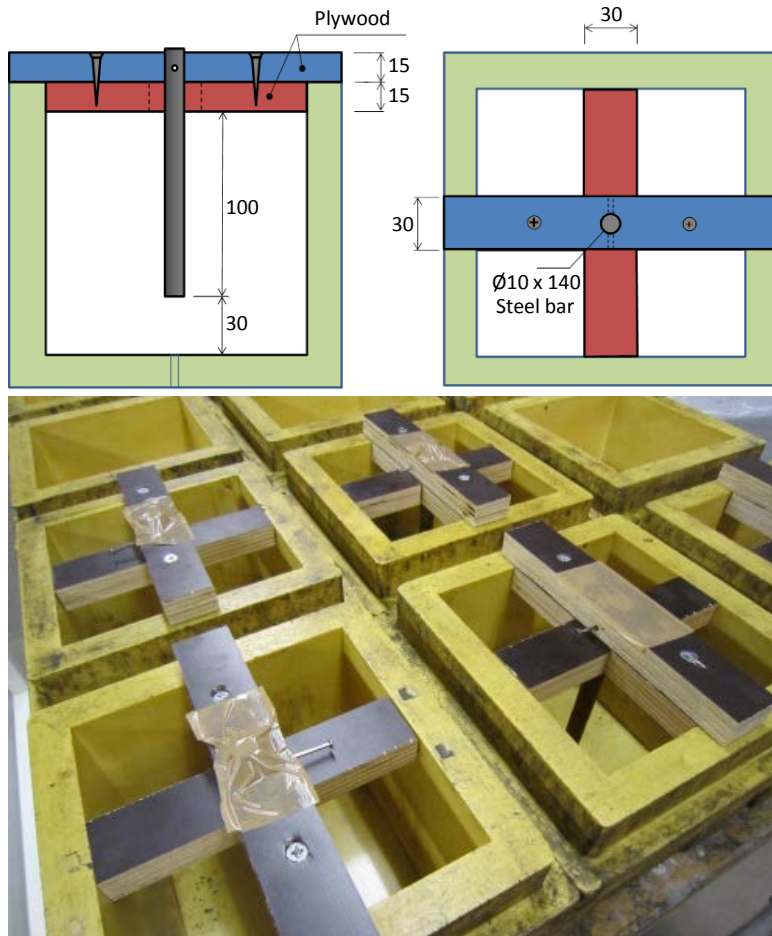


Figure 3.5. Illustration of the mould with correct positioning of the steel bar (dimensions in mm).

After curing in sealed plastic at 20°C for 28 days, the concrete cover was adjusted by diamond saw cutting and the specimens were placed in a chamber for pre-conditioning at 20°C and 23% RH (Figure 3.6) until the chloride penetration by capillary suction (measured in dummies) distanced 3 mm from the steel surface.

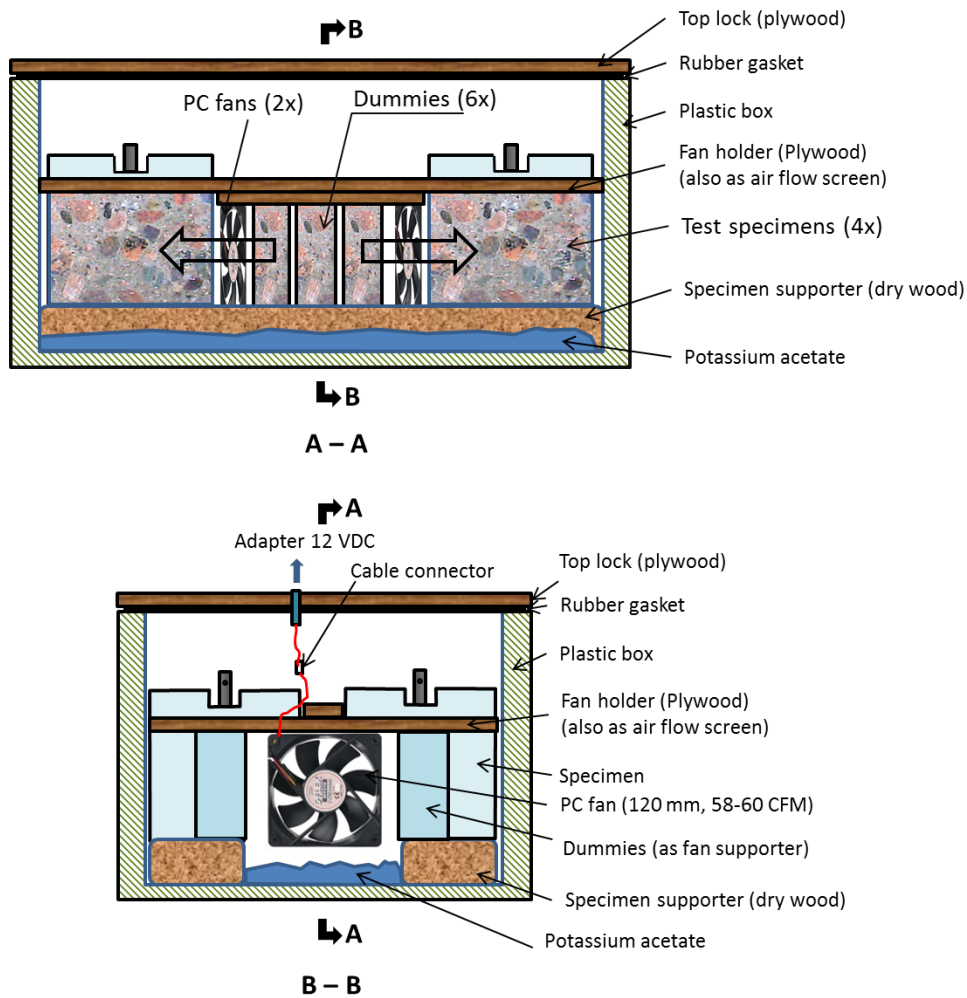


Figure 3.6. Illustration of the preconditioning set-up (RILEM TC 235 CTC 2011).

3.3.2 Methods

Electrochemical treatment

Cathodic current was imposed to the steel bars for 6-7 days to target an accumulated Coulombs value of $8-10 \times 10^6$ C per m^2 of exposed steel surface. The aim was to simulate a service life of 25-30 years under cathodic protection at a current density of about $10 \text{ mA}/m^2$. The experimental setup is schematically represented in Section 2, Figure 2.8; a titanium mesh was used as anode and a 3.3% NaCl solution was used as external electrolyte. The effective Coulombs value of each specimen at the end of the treatment is shown in Table 3.5.

Table 3.5. Coulomb's ($\times 10^6$) value of each specimen under the electrochemical treatment (Paper V).

Specimen	ANL055	ANL045	SCC	FA055	GGBS055	SF055
1ET	8.12	8.06	6.95	12.3	13.2	9.49
2ET	8.95	7.28	7.65	12.1	12.4	7.99

Potential measurement

The specimens were continuously exposed to chloride solution (3.3% NaCl) and the free corrosion potential (E_{corr}) monitored against a manganese dioxide (MnO_2) reference electrode or against an Ag/AgCl gel electrode. All the potentials were expressed vs standard calomel electrode (SCE) using appropriate conversion factors. Depassivation was indicated by a sudden drop in E_{corr} (usually > 150 mV) and the test was terminated. All the specimens were open within less than 1 week after the first signs of depassivation.

Potentiometric titration

Concrete powder was grinded using a diamond tool at a depth of the reinforcement, from two locations according Figure 3.3. The acid-soluble chloride content was determined by potentiometric titration using a chloride selective electrode and 0.01 N AgNO_3 solution as titrant according to AASHTO-T260 (1997). The calcium content was also determined by potentiometric titration using a calcium selective electrode and 0.1 N EDTA solution as titrant (Tang 2003). Because the aggregates used do not contain soluble calcium, the cement or binder content can be estimated. The results were taken as the chloride threshold value (C_{th}), expressed in wt% of binder.

LA-ICP-MS

According to section 3.1.2 LA-ICP-MS was used to analyse the distribution of several elements at a time. In this part of the work, chlorine, calcium, sodium, silica, alumina and iron were qualitatively analysed. The equipment used in this study was a ESI NWR213 (Nd:YAG 213 nm wavelength) laser ablation system coupled to an Agilent 7500 quadrupole inductively coupled plasma mass spectrometer at the department of Earth Sciences, University of Gothenburg. A scan speed of 10 $\mu\text{m/s}$ with a line width of 100 μm was used. It should be stated that in this part of the work, only qualitative profiles were studied. The reason for this was the fact that at some point in this stage of the project, the LA-ICP-MS equipment at Chalmers became disabled. Therefore a solution was to use similar equipment at another university. However, given the limited time availability for utilisation of such equipment, quantitative measurements could not be performed.

4 Results and Discussion

This chapter briefly summarises the main results and discussions from the project. It is divided in three sections, according to the experimental work carried. Section 4.1 is based in Paper I, section 4.2 in Papers II, III and IV and finally section 4.3 is based in Paper V.

4.1 LA-ICP-MS method development

The development of a scanning method that enables the detection of chloride ions in cementitious materials constitutes an important part of the work presented in this thesis. The first step was to assess if LA-ICP-MS was a suitable method for the intended purpose. As such, it was fundamental to optimize the analytical settings of the system in order to guarantee the linearity of the detection. Given the heterogeneous nature of concrete, matrix-matched reference samples are necessary but difficult to produce. In addition, it is necessary to differentiate between cement paste and aggregate grains because chloride is generally bound (or free) in the former. This was accomplished by analysis of concrete powder pellets made from different types of cement. Two types of calibration curves were drawn: between the chloride signal and the chloride content in the sample (Figure 4.1 left) and between the normalized chloride intensity, using calcium as internal standard, and the chloride-to-calcium oxide weight ratio (Figure 4.1 right). While the former approach was proposed for homogeneous samples such as cement paste and mortar containing fine aggregates, the latter is suitable for heterogeneous matrixes such as concrete, allowing estimation of the chloride content per mass of cement. The main factors influencing the stability of the measured element intensities were found to be the surface topography of the sample, the particle size distribution, small fluctuations in laser energy output and possibly, differences in the chloride binding capacity of the cement hydration products. In particular from the results in Figure 4.1 (left) it was found that a finer particle size distribution (series OPC1) influenced the laser sampling characteristics, the flushing efficiency from the ablation cell to the plasma and the ionization efficiency of the particles at the plasma.

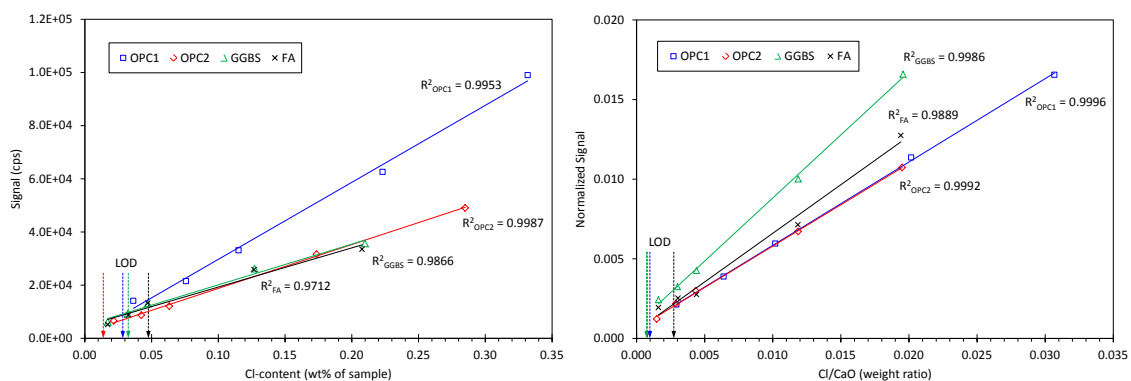


Figure 4.1. Calibration curve for the chloride content in the pellets expressed (left) in wt% of sample and (right) in wt% of cement (Paper I).

The spatial resolution of the method was determined based on the signal decay, after termination of the ablation process, which depends on the flushing efficiency of the system; in

Paper I, at a scan speed of 100 $\mu\text{m/s}$, this was found to be approximately 300-400 μm . Limits of detection can be calculated either using a reference sample that does not contain the analyte or based on the mass spectrum of the blank carrier gas, according to equation 4.1.

$$\text{LOD} = \frac{3s_b - a}{m} \quad (4.1)$$

Here, s_b is the standard deviation of three independent measurements of the blank in counts per second (cps), a is the y-intercept parameter of the calibration curve in cps and m is the slope of the calibration curve in cps/wt%. For all measurements in the present work, limits of detection as low as 0.01 wt% of sample and 0.05 wt% of cement were achieved and regression values close to the unit (>0.97).

Qualitative chloride profiles were measured in cement paste and mortar samples, after diffusion and rapid chloride migration (RCM) tests, respectively. Figure 4.2 shows the results from the RCM test. As mentioned previously, for homogeneous matrixes, it is possible to follow the chloride distributions directly on the sample without the need to apply an internal standard. It was shown that the profiles obtained were in good agreement with those predicted by Tang (1996). Furthermore, the electrical field forces calcium to migrate in the opposite direction leading to differences between the theoretical profile and the one obtained, in particular, when expressed as weight of binder (Figure 4.2 right).

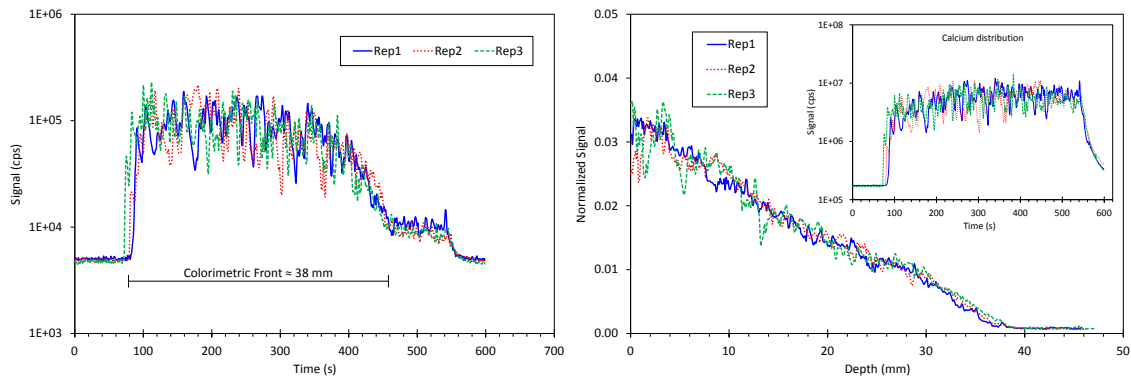


Figure 4.2. Chloride profiles after migration test expressed as (left) total chloride in the sample and (right) normalized distribution of Cl/Ca (Paper I).

Although similar in composition, the physical characteristics of the matrix were distinct; pellets made of pressed concrete powder were found to have different ablation behaviour when compared to hardened cement paste or concrete samples. Therefore it was necessary to validate the results obtained from titration of actual concrete samples using pellets as calibration standard. The following empirical relationship (equation 4.2) was established:

$$\left[\left(\frac{\text{Cl}}{\text{CaO}} \right)_{\text{WR}} \right]_{\text{Titration}} = f \cdot \left[\left(\frac{\text{Cl}}{\text{CaO}} \right)_{\text{WR}} \right]_{\text{LA-ICP-MS}} \quad (4.2)$$

Here $(Cl/CaO)_{WR}$ is the chloride to calcium oxide weight ratio and f is a proportionality factor between potentiometric titration and LA-ICP-MS, $f = 2-3$. This relationship was later applied to the analysis of chloride profiles in concrete (Figure 4.3) where a good agreement with the macro-scale results was found.

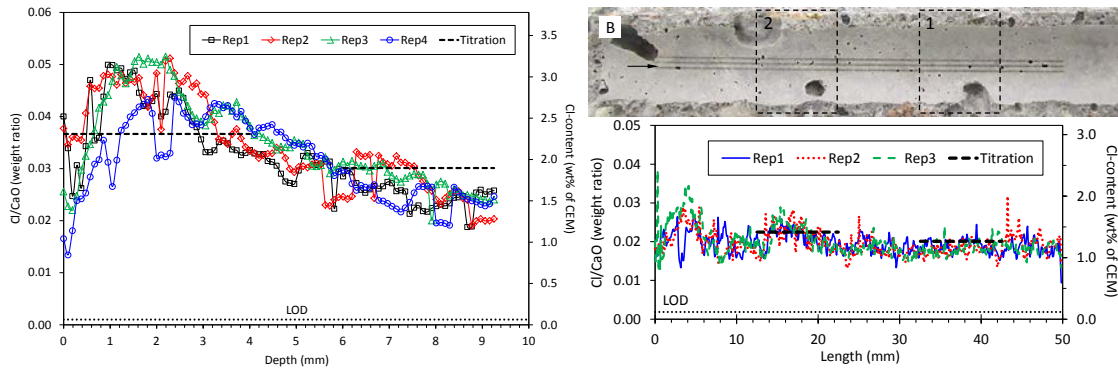


Figure 4.3. Chloride diffusion profiles across the concrete cover (left) and chloride distribution along the concrete-steel interface (right), expressed relative to the cement content (Paper I).

4.2 Chloride distributions and steel surface condition

In Papers II, III and IV, the LA-ICP-MS method developed in section 4.1 was applied to study the chloride induced corrosion phenomena, by mapping the chloride distributions along the concrete-steel interface. Three different surface conditions were investigated, together with the influence of potentiostatic control when compared with free corrosion conditions. It was observed that for all the steel bars that showed signs of corrosion, pitting initiated under submerged conditions. Mainly steel with discontinuous mill-scale corroded and this was usually associated with presence of air voids at the interface. In addition, also cut steel surfaces (stressed) were prone to corrosion. Generally, around the active pits, dark blue/green rust was observed; such corrosion products, formed under low oxygen concentrations, are highly soluble and diffuse into hydroxide or oxygen rich areas lead to the precipitation of $Fe(OH)_2$, followed by oxidation to Fe(III) oxy-hydroxides (goethite, lepidocrocite or akaganeite). Although initially suggested (Paper II) this could not be confirmed in further analysis (Paper IV) by XRD. However, some typical iron oxy-hydroxides and iron-chloride mineral structures were found by SEM studies (Figures 7b and 7c in Paper IV).

Paper II provided an initial valuable insight with regard to chloride distributions around active corrosion sites, where SEM-EDS was used to supplement LA-ICP-MS with semi-quantitative analysis at representative sites along the interface. Despite the differences in the analytical techniques, the results from EDS (Table 2 in Paper II) have shown a good agreement with the chloride distributions obtained by means of LA-ICP-MS (Figure 5 in Paper II). In addition, the meso-scale results (LA-ICP-MS) were compared with the macro-scale chloride contents determined by means of potentiometric titration. It was found that, at the depth of the reinforcement, the chloride content was generally lower than that measured at the corroding sites, since the macro-scale sampling contained a large portion of concrete that may not correspond to that actively corroding; this emphasized the need to evaluate the local chloride concentrations.

With regard to the chloride distributions it was in Paper III suggested that the spatial distribution of aggregates at the front trace of the reinforcement could influence the chloride ingress, and that therefore, at the depth of the reinforcement, the chloride distribution is not homogeneous. However, the elemental distributions obtained from LA-ICP-MS in non-corroded samples indicated that chlorides were relatively homogeneous distributed (Figure 4.4 left) and well correlated with both calcium and iron signals (Papers III and IV). On the other hand, in specimens where corrosion did initiate, the local chloride content at active sites was found to be higher than that measured where the steel remained in its passive condition (Figure 4.4 right). On the light of these observations it was in Paper IV suggested that chloride ions electro-migrate from the relatively large cathodic areas (passive state) to the small anodic areas (active state), due to the electrochemical potential gradient at the steel surface close to the pit. Conversely, calcium ions (from the dissolution of portlandite due to anodic acidification) and soluble iron complexes could be transported away from the anode in a combined mechanism of electro-migration and diffusion, thus explaining the decrease in the calcium intensity often observed around the active sites.

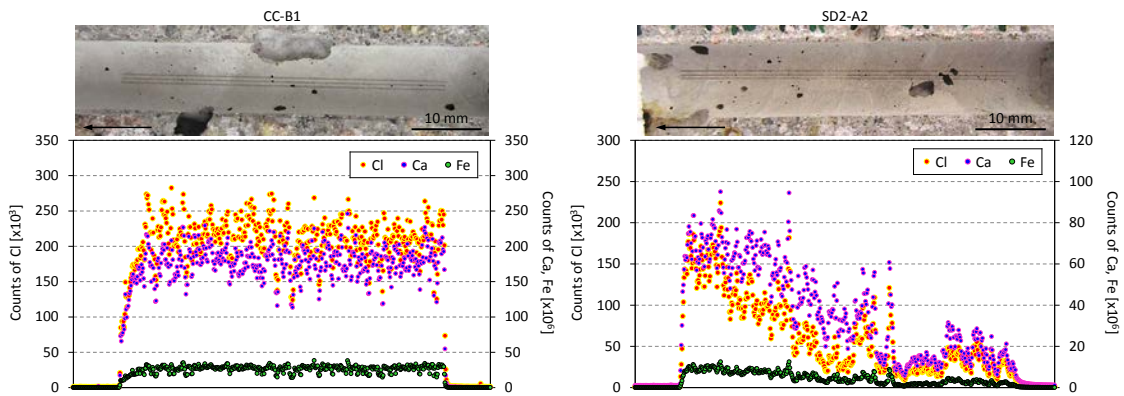


Figure 4.4. Elemental distributions along the concrete-steel interface. The arrows indicate the casting direction (Paper IV).

In this project, the steel surface condition was found to play a significant role on the corrosion onset. As shown in Table 2 in Paper IV, SD type steel bars were more susceptible to pitting corrosion, despite comparable chloride contents at the time to open (Figure 4.5). This has been attributed to discontinuities, cracks and crevices in the mill-scale: it was suggested that these crevices would enhance the formation of microgalvanic cells between the mill-scale and the bare steel, by establishment of potential gradients between adjacent areas of the steel. In a similar way, this could also explain why as-received bars started corroding at interface between the new cut surface and the “old” as-received one, where there might exist a significant electrochemical potential difference. Removal of the heterogeneities, by chemical cleaning the steel, would result in a more homogeneous passive film and hence increased resistance to chloride induced corrosion.

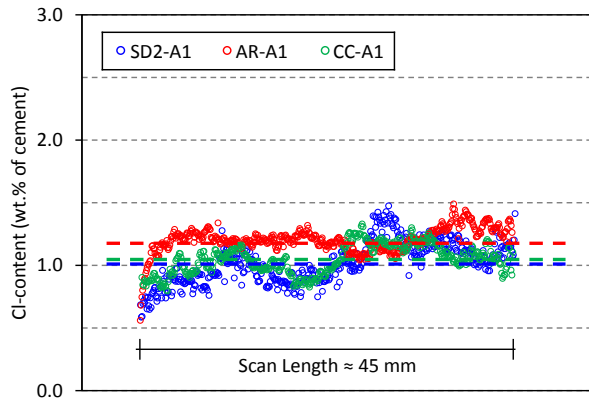


Figure 4.5. Total chloride content profiles along the interface for the different steel surface conditions (Paper IV).

It was early recognized in Papers II and III the importance of defects, such as air voids, at the concrete-steel interface in the corrosion initiation. This was furthermore confirmed in Paper IV where, corrosion initiation for the case of SD type steel bars was associated to the presence of air voids (Table 2 in Paper IV). From the results in Paper IV it was evident that distinction between the influence of the steel surface condition and air voids in the corrosion initiation, is not straightforward and most certainly is the reason for the large differences in the results of threshold value reported in the literature. However, with regard to the mechanism through which air voids can affect the onset of the corrosion it was suggested that these promote the formation of a corrosion cell between the steel covered with hydration products and the contiguous air void. The difference in the oxygen accessibility would mean a difference in the corrosion potential between these two adjacent areas. The potential of the steel within the rich oxygen content area (air void) would then be less negative when compared with that of the covered steel, and thus closer to the pitting potential.

Finally, with regard to differences between tests under open circuit potential and potentiostatic control, the results in Figure 5 - Paper IV indicated that at the time-to-open, the average chloride content along the concrete-steel interface was higher under potentiostatic control than under free corroding conditions. It was suggested that under the influence of anodic polarisation, even if small, it is possible that chloride penetration at the rebar front is through a combined mechanism of diffusion and migration. Therefore, at the time of initiation, the chloride content at the rebar front is likely to be higher than that at the same depth, farther away in the bulk concrete. This could explain why under potentiostatic controlled experiments, lower chloride threshold levels are often measured, a phenomenon that cannot be revealed by traditional concrete sampling methods for chloride analysis.

4.3 Chloride distributions at the time of depassivation

After realising that chlorides accumulated at the anodic sites along the interface, in Paper V an attempt was made to study the chloride distributions along the concrete-steel interface at the first signs of depassivation, in order to try to understand if this effect could occur prior to the initiation of corrosion. In addition, also the effect of the electrochemical treatment prior to testing on the mechanism of chloride induced corrosion and on the C_{th} was investigated.

A total of 24 reinforced concrete specimens were tested, 12 of them were electrochemically treated, corresponding to six different compositions. The free corrosion potential was continuously monitored; as a result of the impressed cathodic current before exposure, electrochemically treated specimens had, in the passive state, a lower potential. At the end of the test period, a total of 20 specimens had shown signs of depassivation by registering a sudden drop in the potential to more negative values (Figure 4.6 left); for all specimens, depassivation was registered as a one-time event and no depassivation-repassivation cycles were observed. However, after depassivation, the potential drop development was somewhat different, with the series containing pozzolanic additions showing a steadier drop when compared with Portland cement concrete (Figure 4.6 right); in particular for the case of SCC, where after splitting of the specimens for visual examination corrosion was sometimes difficult to detect. The reason for this “reluctant” behaviour may be associated to the composition and microstructure of the concrete-steel interface. It is possible that the presence of pozzolanic additions increases the electrical resistivity of the concrete as well as promoting a denser concrete-steel interface. In this situation, the microstructure of the concrete-steel interface plays an important role both in terms of controlling the amount of chloride that is transported to the vicinity of the anodic defective sites before depassivation, as well as in regulating the movement of chloride and hydroxide ions into the pit and diffusion of ferrous ions outwards. After depassivation, the balance between chloride ions and hydroxyl ions in the pit will influence the corrosion rate development. According to Angst et al. (2011a), an increase in the chloride content might be required to prevent repassivation and enable stable pit growth.

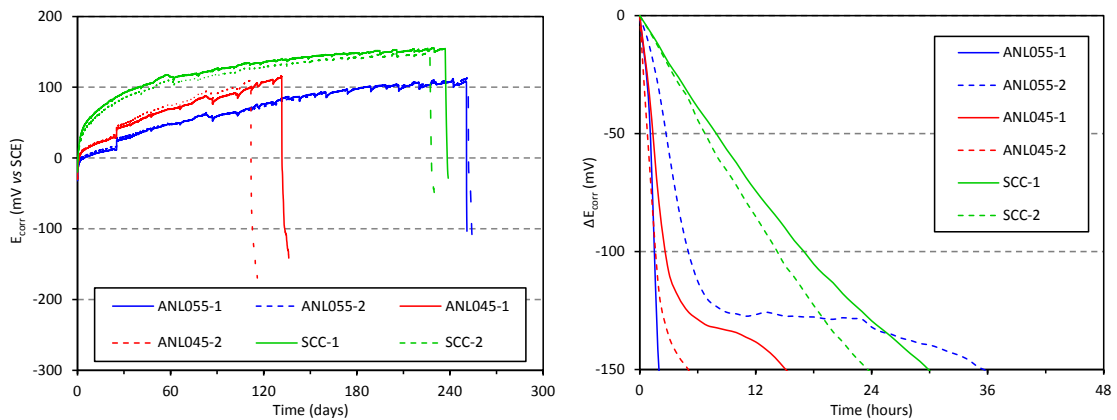


Figure 4.6. (left) Evolution of the open circuit potential and (right) potential drop development after detection of depassivation (Paper V).

In Paper IV it was found that the presence of air voids associated with discontinuities in the mill scale, such as cracks and crevices, could generate differences in the electrochemical activity along the steel surface, i.e. potential gradients, facilitating the corrosion initiation at such locations. The presence of defects in the mill scale can have a detrimental and retarding effect on the formation and performance of the passive film, by limiting the access of oxygen and hydroxyl ions to the metal surface. Furthermore, in the case of air voids, the potential difference between covered steel and steel within the air void is likely to favour the establishment of a corrosion cell. As opposed to the findings reported in Papers II, III and IV, for the series tested in Paper V, the location of corrosion initiation was, in most cases, within

varying range of exposure solution and only seldom, corrosion initiated at air voids. Figure 4.7 shows the typical locations within the interface where corrosion was observed.



Figure 4.7. General aspect of the steel surface and of the concrete-steel interface for specimens: (a) ANL055-1; (b) ANL045-1ET; (c) GGBS055-1 and (d) SF055-2. The arrows indicate the casting direction. Scales in mm (Paper V).

Although in Paper V the steel surface can be considered relatively homogeneous when compared with those studied in Papers II, III and IV and much fewer air voids were present at the concrete-steel interface, potential gradients along the steel surface can also be expected, since the corrosion potential is influenced by a number of factors, as reviewed in Chapter 2. In this regard, of relevance for the discussion in Paper V were the oxygen availability and the effect of the cathodic treatment, on the location of corrosion initiation. It was proposed that, for non-treated samples, the oxygen diffusivity and concentration at the steel surface is higher at the water level than when compared with the fully submerged zone. Since the electrochemical potential is governed by the oxygen availability (dependent on the moisture state) at the steel surface, the higher oxygen partial pressure would shift E_{corr} to values above the pitting potential, favouring the corrosion initiation in this region. In the case of electronically treated specimens, the chloride attack was favoured at the contact zone between the cathodic treated surface and the non-treated anodic zone, further emphasising the importance of potential gradients along the steel surface in the corrosion initiation. Furthermore, these electrochemical differences are likely to be potentiated by differences in the oxygen availability, since also in the case of electronically treated samples, corrosion initiated somewhere within the water level.

A proposed consequence of the formation of potential gradients along the steel surface, with direct impact in the corrosion initiation is the chloride accumulation through a local migration mechanism. One of the major parts of the experimental work carried in this thesis, consisted in the measurement of the chloride distributions along the concrete-steel interface, by means of LA-ICP-MS. In Papers II, III and IV it was found that in the specimens with corrosion-initiated bars, chloride accumulated at the interface surrounding the anode. This effect was attributed to the electromigration of chlorides from passive to active areas within the interface, due to the potential difference between anode and cathode. Thus, in Paper V an attempt was made to study these distributions once depassivation was first detected. In addition, other ions were

also studied. The results (see e.g. Figure 4.8) showed that along active corroding areas of the interface, an increase in chloride was noticeable, even for specimens where the time-to-open was significantly small. Note that all specimens were open within less than one week after depassivation was detected and in some cases within only a few hours, as shown in Table 3 in Paper V. Furthermore, no obvious correlation between the amount of chloride at the anodic sites and the transport factors of ΔE_{corr} and t_{open} was found (Figure 4.9), suggesting that the chloride accumulation at the anodic area had already happened before the sudden potential drop or initiation of pitting corrosion could be registered. From the viewpoint of local chloride migration, the high potential due to oxygen availability attracts the negatively charged chloride ions to this high potential zone and, in turn, the accumulated high chloride concentration leads to a lower pitting potential for the corrosion initiation in this region. This could explain why both treated and non-treated specimens show higher chloride contents at the active corroding sites.

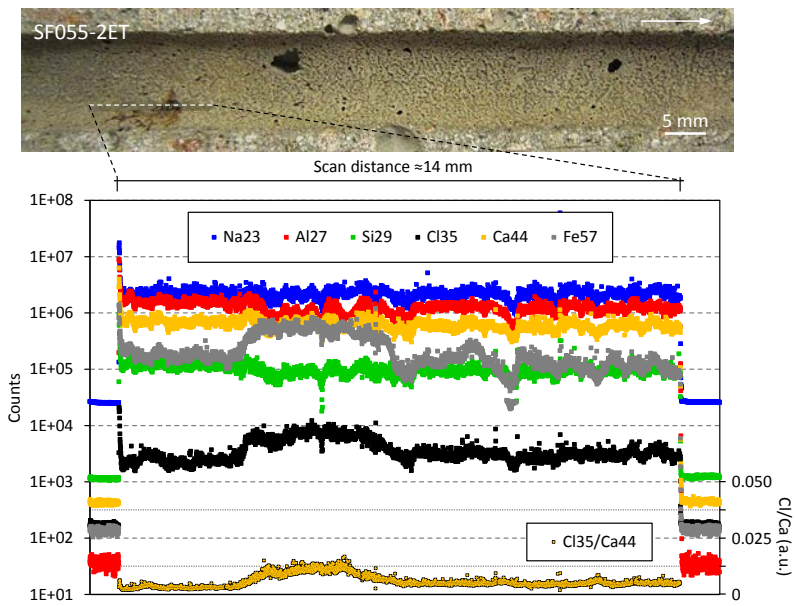


Figure 4.8. Ion distributions along corrosion active sites at the concrete-steel interface for specimen SF055-2ET (Paper V).

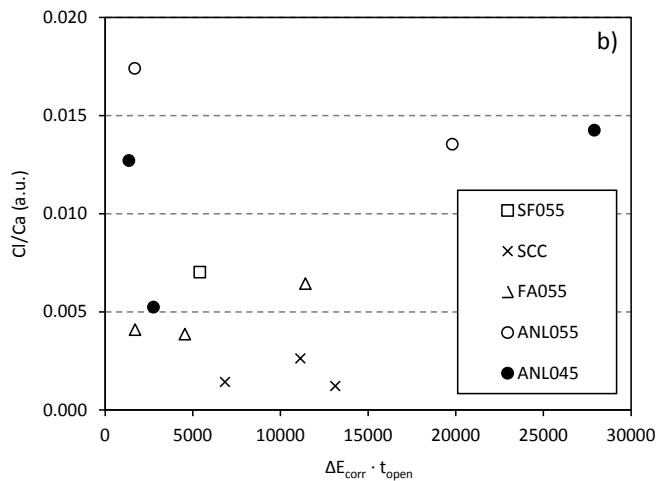


Figure 4.9. Average chloride accumulation along active areas at the concrete-steel interface (Paper V).

Finally, concerning C_{th} , the reduced number of specimens did not allow a proper statistical analysis of the influence of different parameters (namely additions and electrochemical treatment). However, the results obtained could be regarded as C_{th} since the specimens were removed from the test immediately after initiation and clear pits were visible only after just a few hours from opening. The overall scatter was naturally large, ranging from approximately 0.2% to 4% chloride per weight of binder. These values were however, within the range of values reported in the literature. GGBS was found to perform the best, probably because of improved chemical and physical chloride bindings; in this regard it was suggested that hydrotalcite, a product from the high magnesia content in the slag, could play a role. In addition other reasons may contribute to the high resistance of GGBS to chloride induced corrosion, such as the refinement of the pore structure but probably also inhibition of the oxygen cathode reaction due to sulphur deposition at the steel surface, arising from oxidation of sulphide.

5 Conclusions

Chloride induced reinforcement corrosion is one type of highly localized (pitting) corrosion. However, corrosion experiments of steel embedded in concrete, often aim at determining the chloride threshold values (C_{th}), provide information about the chloride content at the cover depth of the bulk concrete but very limited detail in relation to the meso and microstructure. This is particularly true with regard to the chloride distributions at the corrosion active or potentially active sites, at the time of depassivation. In addition, it has been recognized that the two main factors influencing corrosion initiation are the concrete-steel interface and the steel surface condition. In this work, these three aspects of the corrosion process have been experimentally investigated.

The first part of this work consisted in the development of a method that enabled multielement identification in cementitious materials, with high spatial resolution in the scanning mode and at low limits of detection. Therefore, LA-ICP-MS was selected. When compared to more conventional techniques, such as wet chemical analysis or XRF, LA-ICP-MS allows analysis directly on the sample surface, thus significantly reducing sample preparation by eliminating powder sampling procedures and acid digestion. Optimization of the LA-ICP-MS analytical settings and calibration was based on the analysis of concrete powder pellets made of different cement types, for all of which, linearity was observed. Calcium was used as an internal standard allowing expression of the chloride content per weight of cement; this was specially indicated for heterogeneous matrixes such as concrete. At a scan speed of 100 $\mu\text{m/s}$, a spatial resolution of 300-400 μm and limits of detection of 0.05 wt% of cement were determined. Using the pellets as reference samples, the results from LA-ICP-MS were compared to the chloride contents measured by potentiometric titration of representative concrete samples. It was found that LA-ICP-MS underestimated the chloride concentrations because of the difference in surface hardness between the matrices and, in Paper I, an empirical equation was proposed to account for this difference.

The developed LA-ICP-MS method was then applied to study the chloride distributions along the concrete-steel interface. The main purpose was to better understand the role of chloride ions and the influence of the steel surface condition and of the concrete-steel interface on the corrosion initiation. The results have shown that along the interface, a range of chloride concentrations can be expected, with higher values around the corroding active sites. These results were, in Paper II, confirmed by supplementary semi-quantitative studies by means of SEM-EDS. However, measurements in the passive state (Paper IV) indicated that the chloride concentration along the concrete-steel interface was relatively homogeneous. This led, in Paper IV, to the assumption that chlorides accumulated at the anodic regions after corrosion initiation, due to the electrochemical potential gradient between the cathode in the passive state and the anode, actively corroding. Later, measurements immediately after depassivation (Paper V) provided further insight into this local accumulation effect; realising that chloride content at the active regions was not proportional to the time-to-open (Paper V) as it would be expected under the influence of an electrical field, it was suggested that chlorides preferentially accumulate at the anodic regions even prior to depassivation, leading to pitting corrosion.

A local migration mechanism was proposed to account for the chloride build-up around the anode regions. Along the steel, differences in the moisture content and oxygen availability, concentration of aggressive species and metallurgical properties, such as inclusions or mill-scale, are likely to create electrochemical inhomogeneity, i.e. local potential gradients on the passive layer of the steel surface. These differences between more cathodic and anodic regions favour the chloride migration along the interface to the anode regions and the high concentrated chloride ions facilitate the dissolution of the passive film and finally initiate pitting corrosion.

In particular the steel surface condition and the presence of air voids at the concrete-steel interface were recognized as major factors influencing the development of potential gradients along the steel surface. In Paper IV it was found that corrosion initiated almost exclusively for steel bars with inhomogeneous mill-scale and preferentially at air voids locations. In addition, also cut (stressed) surfaces of the steel act as preferential nucleation sites. With regard to air voids, differences in oxygen availability between the steel surface within the air-void and adjacent areas covered with hydration products, are likely to favour the chloride accumulation and establishment of a galvanic cell in the contact zone. In Paper V it was found that corrosion initiated at the contact zone between electronically treated cathode and the non-treated anodic region. The chloride ion distributions along the interface provided further evidence of the influence of the potential gradients between these areas on the local chloride migration.

The microstructure of the concrete-steel interface plays an important role at the early stages of pitting corrosion: before depassivation, by controlling the chloride transport to sites of preferential accumulation and later by regulating the flux of ions in and out of the pit. After the initiation of pitting the corrosion current is mainly governed by the easiness through which the hydroxide ions generated in the cathodic regions flow to the anode (ohmic control) and ions diffuse into and out of the pit (anodic control).

For similar exposure periods, measurements on specimens tested under potentiostatic control have indicated higher chloride concentrations along the concrete-steel interface when compared to specimens kept under free corrosion conditions. The reason for this is still unclear, since under potentiostatic control tests, often lower C_{th} are obtained. It was suggested that under anodic polarisation chloride ingress at the steel surface is not uniform and governed by a combined mechanism of diffusion and migration. Furthermore, this cannot be revealed by traditional bulk chloride measurements.

Finally, with regard to the C_{th} , due to the reduced number of specimens, the results obtained in Paper V do not allow a proper statistical analysis. However, with regard to the test method, the results indicated that, at a macro-scale level, the measured chloride content is representative of the C_{th} , since transition from passive to active state always occurred as a one-time event and no repassivation events were observed.

6 Future Research

The present work addressed the topic of chloride induced corrosion of steel in concrete by investigating qualitatively and semi-quantitatively the chloride distributions along the concrete-steel interface, in order to better understand the corrosion mechanism. LA-ICP-MS has been applied for the purpose, demonstrating further potentialities that had not been explored previously.

With regard to the application of LA-ICP-MS, future work is required in the preparation of standards to enable fully quantitative analysis, improvement of the detection limits and multi-element calibration, as other species (e.g. sulphur, lithium, sodium and potassium) are relevant concerning not only concrete but the general durability of building materials.

Although in the present thesis it was proposed that chlorides accumulate at defective sites at the concrete-steel interface prior to depassivation, it is still uncertain when such accumulation effect takes place. Therefore, further experimental and numerical efforts should be undertaken in order to try to map the chloride build-up at the steel surface. This could provide crucial knowledge concerning the initiation of corrosion.

A great progress has recently been achieved, with the start of the first test trial based on the draft proposal of the RILEM TC 235 CTC involving a number of laboratories. However, concerning the development of a test method for determination of chloride threshold values (C_{th}) in concrete, a couple of questions have been identified from the experience in the present work:

- The sampling area for chloride analysis is not always representative of the level where, along the interface, corrosion is initiated. Thus, it might be necessary adjust the sampling position, in particular when corrosion is observed above the water level;
- Although, under a practical point of view, the actual sampling methods are adequate, there is a need to correlate the chloride concentration at the location sites with that measured at a macro-scale level;
- The present study aimed to reproduce submerged conditions. However as it was observed corrosion initiated often at the water level. Therefore for the same experimental set-up, different exposure conditions (e.g. wet-dry cycles) should be investigated and compared.

Although it now appears consensual that in a test method for determination of C_{th} , the steel should be kept under free corrosion conditions, under a research point of view, the influence of potentiostatic control is still not fully understood and some basic questions are not yet answered:

- Is the composition and microstructure of the passive film, developed under potentiostatic control, the same as that developed under free corrosion conditions?
- Does potentiostatic control influence the microstructure of concrete-steel interface?
- What is the influence of the anodic polarisation, even if small, on the chloride ingress at the interface?

Promising results were obtained for concrete incorporating ground granulated blast furnace slag (GGBS), for both treated and non-treated specimens. It was discussed that the high magnesia content in the slag could effectively increase the chloride binding. In addition, the electrochemical treatment is likely to contribute to the alkali-activation of unreacted slag, due to the production of hydroxyl ions. Therefore further studies should be carried to fully understand and explore the behaviour of GGBS in concrete.

Finally, the efficiency of the electrochemical behaviour is not clear from this project. On the one hand, a decrease in C_{th} was observed for high water-binder ratios (w/b) while on the other hand, even at high w/b, for concrete containing additions, high C_{th} were achieved. Therefore further research should focus on realistic w/b ratios. Furthermore, the effect of such high current densities such as the one applied in the present work is unknown. Thus, in the future, efforts should be made to compare the influence of the current density on the efficiency of the treatment.

From viewpoint of practical applications, research and development of effective methods for reduction of electrochemical potential difference on the steel surface may significantly elevate chloride threshold for corrosion initiation and consequently improve the service life of reinforced concrete structures exposed to chloride environment.

7 References

- AASHTO-T260 (1997) Standard method of test for sampling and testing for chloride ion in concrete and concrete raw materials, American Association of State Highway and Transportation Officials.
- Al Khalaf MN and Page CL (1979) Steel/mortar interfaces: microstructural features and modes of failure, *Cement and Concrete Research* 9 (2) 197-208.
- Alekseev SN (1993) Corrosion of steel reinforcement, in *Durability of reinforced concrete in aggressive media*, edited by S.K. Mallick, Balkema/Rotterdam/Brookfield, pp. 305-349.
- Alonso C, Castellote M and Andrade C (2002) Chloride threshold dependence of pitting potential of reinforcements, *Electrochimica Acta* 47 (21) 3469-3481.
- Alonso MC and Sanchez M (2009) Analysis of the variability of chloride threshold values in the literature, *Materials and Corrosion* 60 (8) 631-637.
- Alvarez MG and Galvele JR (1984) The mechanism of pitting of high purity iron in NaCl solutions, *Corrosion Science* 24 (1) 27-48.
- Andrade C and Castellote M (2002) Recommendation of RILEM TC 178-TMC: testing and modelling chloride penetration in concrete - analysis of total chloride content in concrete, *Materials and Structures* 35 (9) 583-585.
- Angst U (2011) Chloride induced reinforcement corrosion in concrete - Concept of critical chloride content - methods and mechanisms, PhD Thesis, NTNU, Trondheim, Norway.
- Angst U and Vennesland Ø (2009) Detecting critical chloride content in concrete using embedded ion selective electrodes - effect of liquid junction and membrane potentials, *Materials and Corrosion* 60 (8) 638-643.
- Angst U, Elsener B, Larsen CK and Vennesland Ø (2009a) Critical chloride content in reinforced concrete - A review, *Cement and Concrete Research* 39 (12) 1122-1138.
- Angst U, Vennesland Ø and Myrdal R (2009b) Diffusion potentials as source of error in electrochemical measurements in concrete, *Materials and Structures* 42 (3) 365-375.
- Angst U, Elsener B, Myrdal R and Vennesland Ø (2010) Diffusion potentials in porous mortar in a moisture state below saturation, *Electrochimica Acta* 55 (28) 8545-8555.
- Angst U, Elsener B, Larsen CK and Vennesland Ø (2011a) Chloride induced reinforcement corrosion: Electrochemical monitoring of initiation stage and chloride threshold values, *Corrosion Science* 53 (4) 1451-1464.
- Angst U, Elsener B, Larsen CK and Vennesland Ø (2011b) Defects at the steel/concrete interface and their influence on chloride induced reinforcement corrosion, *Cement and Concrete Research* (submitted).
- Ann KY and Song H-W (2007) Chloride threshold level for corrosion of steel in concrete. *Corrosion Science* 49 (11) 4113-4133.

- Arliguie G, Castel A, Vidal T and François R (2003) Influence of steel-concrete interface quality on reinforcement corrosion induced by chlorides, *Magazine of Concrete Research* 55 (2) 151-159.
- Arup H and Sørensen HE (1995) A proposed technique for determining chloride thresholds, in *Proceedings of Chloride penetration into concrete*, International RILEM workshop, Saint-Rémy-les-Chevreuse, France, pp. 460-469.
- Arup H (1983) The mechanisms of protection of steel by concrete, in *Corrosion of Reinforcement in Concrete Construction*, edited by A.P. Crane, Society of chemical industry, Ellis Horwood Limited, pp. 151-157.
- Ban VS, Volodin BL and Dolgi S (2011) Determination of chloride ion concentrations in concrete by means of near-infrared spectrometry, *Nondestructive Characterization for Composite Materials, Aerospace Engineering, Civil Infrastructure and Homeland Security 2011*, edited by H. Felix Wu, *Proc. of SPIE Vol. 7983, 798324*, pp.1-7.
- Bardal E (2004) *Corrosion and protection, Engineering Materials and Processes*, 1st edition, Springer, London, UK.
- Bentur A, Diamond S and Berke NS (1997) *Steel Corrosion in Concrete: Fundamentals and Civil Engineering Practice*, E&FN Spon.
- Bertolini L and Redaelli E (2009) Depassivation of steel reinforcement in case of pitting corrosion: detection techniques for laboratory studies, *Materials and Corrosion* 60 (8) 608-616.
- Bertolini L, Elsener B, Pedeferri P and Polder R (2004) *Corrosion of steel in concrete - prevention, diagnosis and repair*, 1st edition, Wiley-VCH, Weinheim, Germany.
- Bertolini L, Bolzoni F, Gastaldi M, Pastore T, Pedeferri P and Redaelli E (2009) Effects of cathodic prevention on the chloride threshold for steel corrosion in concrete, *Electrochimica Acta* 54 (5) 1452-1463.
- Boubitsas D, Tang L (2012) The influence of reinforcement steel surface condition on initiation of chloride induced corrosion, *Materials and Corrosion* (submitted).
- Boulyga SF and Heumann KG (2005) Direct determination of halogens in powdered geological and environmental samples using isotope dilution laser ablation ICP-MS, *International Journal of Mass Spectrometry* 242 (2-3) 291-296.
- Buenfeld N, Glass G, Reddy B and Viles F (2004) Process for the protection of reinforcement in reinforced concrete, United States Patent 6685822, USPTO, Alexandria, VA, USA.
- Burakov VS, Kiris VV and Raikov SN (2007) Optimization of conditions for spectral determination of chlorine content in cement-based materials, *Journal of Applied Spectroscopy* 74 (3) 321-327.
- Byfors K (1987) Influence of silica fume and fly ash on chloride diffusion and pH values in cement paste, *Cement and Concrete Research* 17 (1) 115-130.
- Carugati G, Rauch S and Kylander ME (2010) Experimental assessment of a large sample cell for laser ablation-ICP-MS and its application to sediment core micro-analysis, *Microchimica Acta* 170 (1-2) 39-45.

- Chaussadent T and Arliguie G (1999) AFREM test procedures concerning chlorides in concrete: extraction and titration methods, *Materials and Structures* 32 (3) 230-234.
- Cheng A, Huang R, Wu J-K and Chen C-H (2005) Influence of GGBS on durability and corrosion behaviour of reinforced concrete, *Materials Chemistry and Physics* 93 (2-3) 404-411.
- Cheng YF and Luo JL (1999) Metastable pitting of carbon steel under potentiostatic control, *Journal of The Electrochemical Society* 146 (3) 970-976.
- Climent MA, Viqueira E, de Vera G and López-Atalaya MM (1999) Analysis of acid-soluble chloride in cement, mortar, and concrete by potentiometric titration without filtration steps, *Cement and Concrete Research* 29 (6) 893-898.
- Colleparidi M, Marcialis A and Turriziani R, (1972) Penetration of chloride ions into cement pastes, *Journal of the American Ceramic Society* 55 (10) 534-535.
- de Rooij MR and Polder R (2005) Probabilistic approach for local chloride heterogeneity near reinforcement, in *Application of Codes, Design and Durability Regulations*, 6th International Congress, Theme Two: Service Life and Durability Design, University of Dundee, Scotland, UK.
- Dejke V (2001) Durability of FRP reinforcement in concrete - literature review and experiments, Publication P-01:1, CTH, Göteborg, Sweden.
- Delagrave A, Bigas JP, Ollivier JP, Marchand J and Pigeon M (1997) Influence of the interfacial zone on the chloride diffusivity of mortars, *Advanced Cement Based Materials* 5 (3) 86-92.
- Dhir RK, Jones MR and Ahmed HE (1990) Determination of total and soluble chlorides in concrete, *Cement and Concrete Research* 20 (4) 579-590.
- Elsener B, Andrade C, Gulikers J, Polder R and Raupach M (2003) Half-cell potential measurements - Potential mapping on reinforced concrete structures, *Materials and Structures* 36 (7) 461-471.
- European Standard EN196-21 (1989) Methods for testing cement: determination of the chloride, carbon dioxide and alkali content of cement, European Committee for Standardization.
- Feng X, Thomas MDA, Bremner TW, Folliard KJ and Fournier B (2010) New observations on the mechanism of lithium nitrate against alkali silica reaction (ASR), *Cement and Concrete Research* 40 (1) 94-101.
- François R and Arliguie G (1998) Influence of service cracking on reinforcement steel corrosion, *Journal of Materials in Civil Engineering* 10 (1) 14-20.
- Gastel M, Becker JS, Küppers G and Dietze H-J (1997) Determination of long-lived radionuclides in concrete matrix by laser ablation inductively coupled plasma mass spectrometry, *Spectrochimica Acta Part B: Atomic Spectroscopy* 52 (14) 2051-2059.
- Ghods P, Isgor OB, McRae GA, Li J and Gu GP (2011) Microscopic investigation of mill scale and its proposed effect on the variability of chloride-induced depassivation of carbon steel rebar, *Corrosion Science* 53 (3) 946-954.

- Ghods P, Isgor OB, McRae G and Miller T (2009) The effect of concrete pore solution composition on the quality of passive oxide films on black steel reinforcement, *Cement & Concrete Composites* 31 (1) 2-11.
- Glass GK and Buenfeld NR (1997) The presentation of the chloride threshold level for corrosion of steel in concrete, *Corrosion Science* 39 (5) 1001-1013.
- Gui J and Devine TM (1994) The influence of sulfate ions on the surface enhanced Raman spectra of passive films formed on iron, *Corrosion Science* 36 (3) 441-462.
- Günther D and Hattendorf B (2005) Solid sample analysis using laser ablation inductively coupled plasma mass spectrometry, *Trends in Analytical Chemistry* 24 (3) 255-265.
- Halamickova P, Detwiler RJ, Bentz DP and Garboczi EJ (1995) Water permeability and chloride ion diffusion in portland cement mortars: Relationship to sand content and critical pore diameter, *Cement and Concrete Research* 25 (4) 790-802.
- Hansson CM (1984) Comments on electrochemical measurements of the rate of corrosion of steel in concrete, *Cement and Concrete Research* 14 (4) 574-584.
- Hartt WH and Nam J (2008) Effect of cement alkalinity on chloride threshold and time-to-corrosion of reinforcing steel in concrete, *Corrosion* 64 (8) 671-680.
- Horne AT, Richardson IG and Brydson RMD (2007) Quantitative analysis of the microstructure of interfaces in steel reinforced concrete, *Cement and Concrete Research* 37 (12) 1613-1623.
- Hunkeler F (2005) *Corrosion in reinforced concrete structures*, edited by Hans Böhni, Woodhead Publishing, Cambridge, England.
- Ito K, Hasebe N, Sumita R, Arai S, Yamamoto M, Kashiwaya K and Ganzawa Y (2009) LA-ICP-MS analysis of pressed powder pellets to luminescence geochronology, *Chemical Geology* 262 (3-4) 131-137.
- Jaffer SJ and Hansson CM (2009) Chloride-induced corrosion products of steel in cracked-concrete subjected to different loading conditions, *Cement and Concrete Research* 39 (2) 116-125.
- Jensen OM, Hansen PF, Coats AM and Glasser FP (1999) Chloride ingress in cement paste and mortar, *Cement and Concrete Research* 29 (9) 1497-1504.
- Jensen OM, Coats AM and Glasser FP (1996) Chloride ingress profiles measured by electron probe micro analysis, *Cement and Concrete Research* 26 (1) 1695-1705.
- Justnes H (1998) A review of chloride binding in cementitious systems, *Nordic Concrete Research*, Nordic Concrete Federation, Publication No.21, pp. 48-63.
- Küter A (2009) *Management of reinforcement corrosion - A thermodynamic approach*, PhD Thesis, DTU, Copenhagen, Denmark.
- Li L and Sagues AA (2001) Chloride corrosion threshold of reinforcing steel in alkaline solutions - open-circuit immersion tests, *Corrosion* 57 (1) 19-28.

- Lin B, Hu R, Ye C, Li Y and Lin C (2010) A study on the initiation of pitting corrosion in carbon steel in chloride-containing media using scanning electrochemical probes, *Electrochimica Acta* 55 (22) 6542-6545.
- MacDougall B and Graham MJ (2002) Growth and stability of Passive films, in *Corrosion Mechanisms in Theory and Practice*, 2nd edition (P. Marcus), Marcel Dekker Inc., New York, USA.
- Mahallati E and Saremi M (2006) An assessment on the mill scale effects on the electrochemical characteristics of steel bars in concrete under DC-polarization, *Cement and Concrete Research* 36 (7) 1324-1329.
- Mangat PS and Molloy BT (1994) Prediction of long term chloride concentration in concrete, *Materials and Structures* 27 (6) 338-346.
- Marcotte TD (2001) Characterization of chloride-induced corrosion products that form in steel-reinforced cementitious materials, PhD Thesis, University of Waterloo, Waterloo, Canada.
- Mietz J (1998) Electrochemical rehabilitation methods for reinforced concrete structures, *European Federation of Corrosion Publications* 24, London, UK.
- Mohammed T, Otsuki N, Hisada M, and Shibata T (2001) Effect of crack width and bar type on corrosion of steel in concrete, *Journal of Materials in Civil Engineering* 13 (3) 194-201.
- Mohammed TU and Hamada H (2001) A discussion of the paper "Chloride threshold values to depassivate reinforcing bars embedded in a standardized OPC mortar" by C. Alonso, C. Andrade, M. Castellote and P. Castro, *Cement and Concrete Research* 31 (5) 835-838.
- Monteiro PJM, Gjrv OE and Mehta PK (1985) Microstructure of the steel-cement paste interface in the presence of chloride, *Cement and Concrete Research* 15 (5) 781-784.
- Montemor MF, Simes AMP and Ferreira MGS (1998) Analytical characterization of the passive film formed on steel in solutions simulating the concrete interstitial electrolyte, *NACE Corrosion* 54 (5) 347-353.
- Mori D, Yamada K, Hosokawa Y and Yamamoto M (2006) Applications of electron probe microanalyzer for measurement of Cl concentration profile in concrete, *Journal of Advanced Concrete Technology* 4 (3) 369-383.
- Nagataki S, Otsuki N, Wee TH and Nakashita K (1993) Condensation of chloride ions in hardened cement matrix materials and on embedded steel bars, *ACI Materials Journal*, 90 (4) 323-332.
- Neville AM (1995) *Properties of concrete*, 4th Edition, Longman, Essex, UK.
- Nielsen PE and Geiker MR (2003) Chloride diffusion in partially saturated cementitious material, *Cement and Concrete Research* 33 (1) 133-138.
- Nilsson L-O, Poulsen E, Sandberg P, Srensen HE and Klinghoffer O (1996) Chloride penetration into concrete - State of the art: Transport processes, corrosion initiation, test methods and prediction models, HETEK Report No.53, Danish Road Directorate, Copenhagen, Denmark.

- Nilsson L-O (2009) Models for chloride ingress into concrete - from Collepardi to today, *International Journal of Modelling, Identification and Control* 7 (2) 129-134.
- Nygaard PV and Geiker MR (2005) A method for measuring the chloride threshold level required to initiate reinforcement corrosion in concrete, *Materials and Structures* 38 (4) 489-494.
- Page CL (1975) Mechanism of corrosion protection in reinforced concrete marine structures, *Nature* 258, 514-515.
- Page CL (2009) Initiation of chloride-induced corrosion of steel in concrete: role of the interfacial zone, *Materials and Corrosion* 60 (8) 586-592.
- Page CL and Treadaway KWJ (1982) Aspects of the electrochemistry of steel in concrete, *Nature* 297, 109-115.
- Pedefferri P (1992) Cathodic protection of new concrete constructions, in *Proceedings of the International Conference on Structural Improvement through Corrosion Protection of Reinforced Concrete*, Institute of Corrosion, London.
- Pickering HW and Frankenthal RP (1972) On the mechanism of localised corrosion of iron and stainless steel, *Journal of The Electrochemical Society* 119 (10) 1297-1304.
- Pillai RG and Trejo D (2005) Surface condition effects on critical chloride threshold of steel reinforcement, *ACI Materials Journal* 102 (2) 103-109.
- Polder R (2003) Electrochemical maintenance methods, in *Corrosion of steel in reinforced concrete structures*, Final report COST Action 521.
- Potgieter SS and Marjanovic L (2007) A further method for chloride analysis of cement and cementitious materials - ICP-OES, *Cement and Concrete Research* 37 (8) 1172-1175.
- Potgieter S, Potgieter J and Panicheva S (2004) Investigation into methods of chloride analysis of South African cement and cement-related materials with low chloride concentrations, *Materials and Structures* 37 (3) 155-160.
- Pourbaix M (1974) Applications of electrochemistry in corrosion science and practice, *Corrosion Science* 14 (1) 25-82.
- Pourbaix M (1963) *Atlas d'équilibres électrochimiques*, Centre Belge d'Etude de la Corrosion CEBELCOR / Gauthier-Villars & Cie, Paris.
- Poursaee A and Hansson CM (2009) Potential pitfalls in assessing chloride-induced corrosion of steel in concrete, *Cement and Concrete Research* 39 (5) 391-400.
- Proverbio E and Carassiti F (1997) Evaluation of chloride content in concrete by X-ray fluorescence, *Cement and Concrete Research* 27 (8) 1213-1223.
- Refait Ph and Génin J-MR (1993) The oxidation of ferrous hydroxide in chloride-containing aqueous media and Pourbaix diagrams of green rust one, *Corrosion Science* 34 (5) 797-819.
- RILEM TC 235 CTC (2011) Technical committee "Corrosion initiating chloride threshold concentrations in concrete", www.rilem.net, activity started in 2009.

- Russo RE, Mao X and Borisov OV (1998) Laser ablation sampling, *Trends in Analytical Chemistry* 17 (8-9) 461-469.
- Ryou JS and Ann KY (2008) Variation in the chloride threshold level for steel corrosion in concrete arising from different chloride sources, *Magazine of Concrete Research* 60 (3) 177-187.
- Sandberg P (1995) Critical evaluation of factors affecting chloride initiated reinforcement corrosion in concrete, Report TVBM-3068, LTH, Lund, Sweden.
- Sandberg P (1998) Chloride initiated reinforcement corrosion in marine concrete, Report TVBM-1015, LTH, Lund, Sweden.
- Strehblow H-H (2002) Mechanisms of Pitting Corrosion, in *Corrosion Mechanisms in Theory and Practice*, 2nd edition (P. Marcus), Marcel Dekker Inc., New York, USA.
- Söylev TA and François R (2003) Quality of steel-concrete interface and corrosion of reinforcing steel, *Cement and Concrete Research* 33 (9) 1407-1415.
- Tang L (1996) Chloride transport in concrete - measurement and prediction, Publication P-96:6, Department of Building Materials, Chalmers University of Technology, Göteborg, Sweden.
- Tang L (2003) Report 2003:07, Swedish National Testing and Research Institute, Borås, Sweden.
- Tang L and Nilsson L-O (1992) Chloride diffusivity in high strength concrete at different ages, *Nordic Concrete Research*, Nordic Concrete Federation, Publication No. 11, pp. 162-171.
- Tang L, Utgenannt P, Lindvall A and Boubitsas D (2012) Validation of models and test methods for assessment of durability of concrete structures in the road environment, CBI Report 2:2012.
- Takewaka K and Matsumoto S (1988) Quality and cover thickness of concrete based on the estimation of chloride penetration in marine environments, in *Proceedings of 2nd International Conference of Concrete in Marine Environment*, edited by V.M. Malhotra, ACI SP-109, pp. 381-400.
- Taylor HE (2001) *Inductively Coupled Plasma Mass Spectrometry: Practices and Techniques*, Academic Press.
- Tuutti K (1982) Corrosion of steel in concrete, CBI Report 4:82.
- Veleva L, Alpuche-Aviles MA, Graves-Brook MK and Wipf DO (2002) Comparative cyclic voltammetry and surface analysis of passive films grown on stainless steel 316 in concrete pore model solutions, *Journal of Electroanalytical Chemistry* 537 (2-3) 85-93.
- Vennesland Ø, Raupach M and Andrade C (2007) Recommendation of RILEM TC 154-EMC: Electrochemical techniques for measuring corrosion in concrete - measurements with embedded probes, *Materials and Structures* 40 (8) 745-758.
- Verink ED and Pourbaix M (1971) Pitting potentials versus pH, *Corrosion* 27, 495.
- Wall H and Nilsson L-O (2008) A study on sampling methods for chloride profiles: simulations using data from EPMA, *Materials and Structures* 41 (7) 1275-1281.

- Webb EG, Paik CH, Alkire RC (2001) Local detection of dissolved sulfur species from inclusions in stainless steel using Ag microelectrode, *Electrochemistry and Solid-State Letters* 4 (4) B15-B18.
- Wilsch G, Weritz F, Schaurich D and Wiggemhauser H (2005) Determination of chloride content in concrete structures with laser-induced breakdown spectroscopy, *Construction and Building Materials* 19 (10) 724-730.
- Win PP, Watanabe M and Machida A (2004) Penetration profile of chloride ion in cracked reinforced concrete, *Cement and Concrete Research* 34 (7) 1073-1079.
- Yonezawa T, Ashworth V and Procter RPM (1988) Pore solution composition and chloride effects on the corrosion of steel in concrete, *Corrosion* 44 (7) 489-499.
- Yu H and Hartt WH (2007) Effects of reinforcement and coarse aggregates on chloride ingress into concrete and time-to-corrosion: Part 1 - Spatial chloride distribution and implications, *Corrosion* 63 (9) 843-849.
- Yu H, Himiob RJ and Hartt WH (2007) Effects of reinforcement and coarse aggregates on chloride ingress into concrete and time-to-corrosion: Part 2 - Spatial distribution of coarse aggregates, *Corrosion* 63 (10) 924-931.
- Yu H, Shi X, Hartt WH and Lu B (2010) Laboratory investigation of reinforcement corrosion initiation and chloride threshold content for self-compacting concrete, *Cement and Concrete Research* 40 (10) 1507-1516.
- Zhang R, Castel A and François R (2011) Influence of steel-concrete interface defects owing to the top-bar effect on the chloride-induced corrosion of reinforcement, *Magazine of Concrete Research* 63 (10) 773-781.